

## 40th Western Protective Relay Conference, 2013

# How Distance Relays Are Impacted by Pre-fault Power Flow On Detection Of Resistive Faults An Impedance Loci Based Study

Sinan Saygin, GE Digital Energy, Carlsbad, CA, USA  
Zhiying Zhang, Iliia Voloh, GE Digital Energy, Markham, ON, Canada

### 1. Introduction

Ideally distance relays are designed to measure the line positive sequence impedance from the relay location to the point of fault. There are many factors that conspire against a realization of such an ideal distance relay. Load flow coupled with fault arc resistance / ground fault impedance can result in overreach and underreach of distance relays and may result in misoperations in some cases.

Furthermore, high resistance ground faults need to be seen and cleared as much as possible with distance relays and if not, with complementary directional ground fault schemes. On the other hand, with modern distance relays we have the option of choosing operating characteristics that would provide increased sensitivity and security. Sensitivity here refers to coverage of ground faults with high resistance values fed from different sources from the two ends, and security, to confining the relay operation only to the protected zone during external faults and unfaulted system conditions including abnormal operating conditions and power swings.

The object of the paper is to calculate impedances seen by distance relays during various fault and operating conditions as a function of the working impedance (prefault impedance seen by the relay) and the value of the fault resistance. The term "Working Impedance" is taken from a paper of J. Zydanowicz (Ref. 1).

First, a method is developed for calculation of apparent impedances seen by distance relays during ground faults. It is shown that; as fault resistance varies from 0 to infinity the locus of impedance seen by the relay describes an arc of a circle on the R-X plane, with one pole at the point of the fault of the protected line ( $z_{1m}$ , pole L) and the other on the working impedance (Z, pole K). The centers and radii of the arches are calculated and loci are drawn for different operating and fault conditions.

The relation between the "Swing Angle" (angle between two equivalent sources at terminals of the system) and the working impedance is taken into account in loci calculations. The studies are carried out for two different source conditions; "Equal Infeed" and "Weak (local) Infeed".

## 2. Phase to ground fault analysis

The connection of sequence networks for a phase to ground fault is shown in Figure 1,  $E_L$  and  $E_R$  represent the equivalent sources behind the local and remote ends of the line with their respective source impedances  $Z_{SL}$  and  $Z_{SR}$ .

### 2.1 Components of the fault currents

According to superimposition theorem we can represent fault currents as sum of the currents before the fault ( $I_{pf}$ , pre fault current) and the superimposed currents, ( $\Delta I$ ), due to fault only.

Superimposed currents can be calculated by replacing the voltage sources in the positive sequence network by an equivalent source at the fault point, with a value of pre-fault voltage at this point, but of opposite polarity, in series with an impedance,  $Z_{fault}$ , comprising the fault resistance and negative and zero sequence impedance networks as appropriate to the type of fault, as shown in Figure 2.

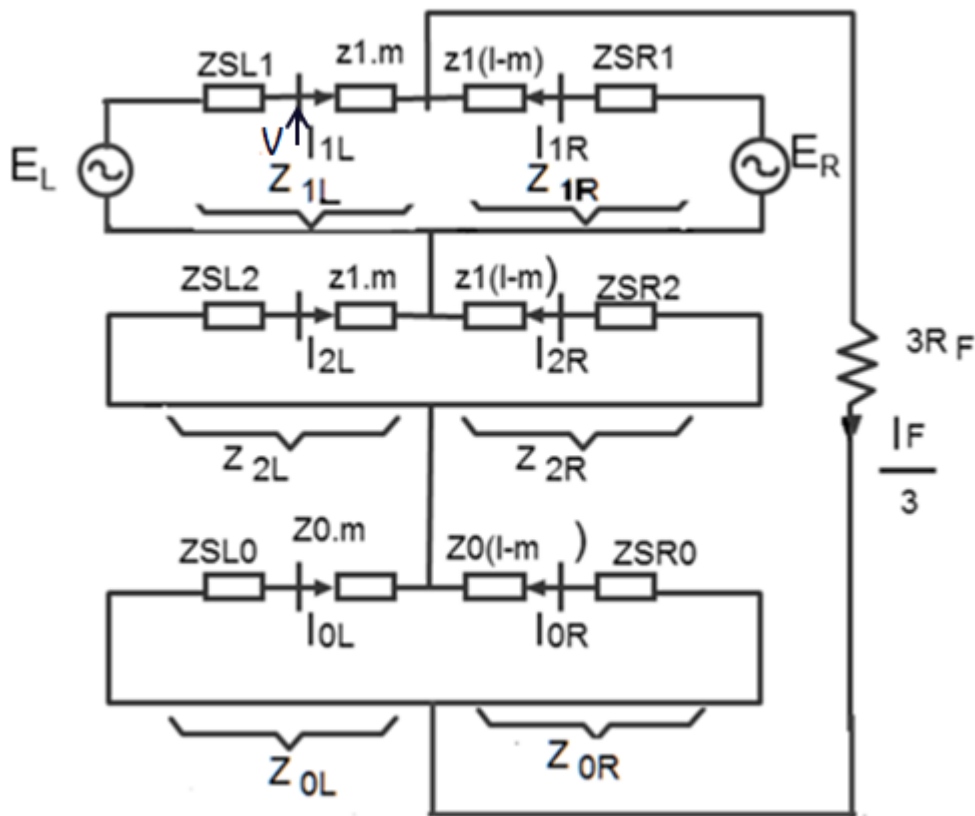


Figure 1: Connection of Sequence Networks for a Phase to Ground Fault.

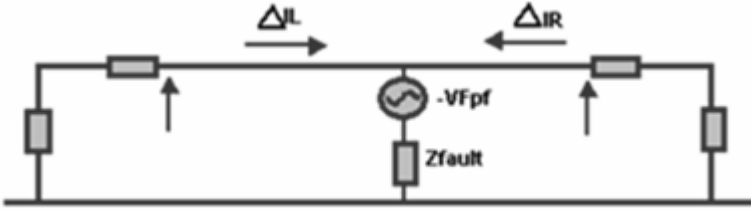


Figure 2: Superimposition Theorem Applied to the Positive Sequence Network.

Therefore, we can express local and remote currents as;

$$I_L = I + \Delta I_{1L} \quad (1)$$

$$I_R = -I + \Delta I_{1R} \quad (2)$$

Where;

$I$  = pre-fault current.

The total fault current  $I_F$  is obtained as;

$$I_F = I_L + I_R = \Delta I_L + \Delta I_R$$

The superimposed network connection of the sequence networks for the phase to ground fault is shown in Figure 3.

## 2.2 Calculation of $Z_R$ , impedance measured by the distance relay

The voltage applied to the distance relay with a ground fault can be expressed as;

$$V_A = (I_A + k_0 \cdot I_0)z_{1.m} + I_F \cdot R_F$$

And the impedance measured by the relay,  $Z_{LR}$  is;

$$Z_{LR} = z_{1.m} + \frac{I_F \cdot R_F}{I_A + k_0 \cdot I_0} \quad (3)$$

Where we can define the Apparent Resistance (Fault resistance as measured by the relay);

$$R_{app} = \frac{I_F \cdot R_F}{I_{AL} + k_0 \cdot I_{0L}} \quad (4)$$

From the superimposed network;

$$I_{1L} = I + \Delta I_{1L}$$

$$I_{1R} = -I + \Delta I_{1R}$$

And;

$$I_A = (I + \Delta I_{1L}) + I_{2L} + I_{0L}$$

Substituting;

$$R_{app} = \frac{(I_F \cdot R_F)}{I + (\Delta I_{1L} + I_{2L} + I_{0L}) + k_0 \cdot I_{0L}} \quad (5)$$

From Figure 3;

$$I_F = 3(V_L - I_{pf} \cdot z_{1m}) / Z_{total}$$

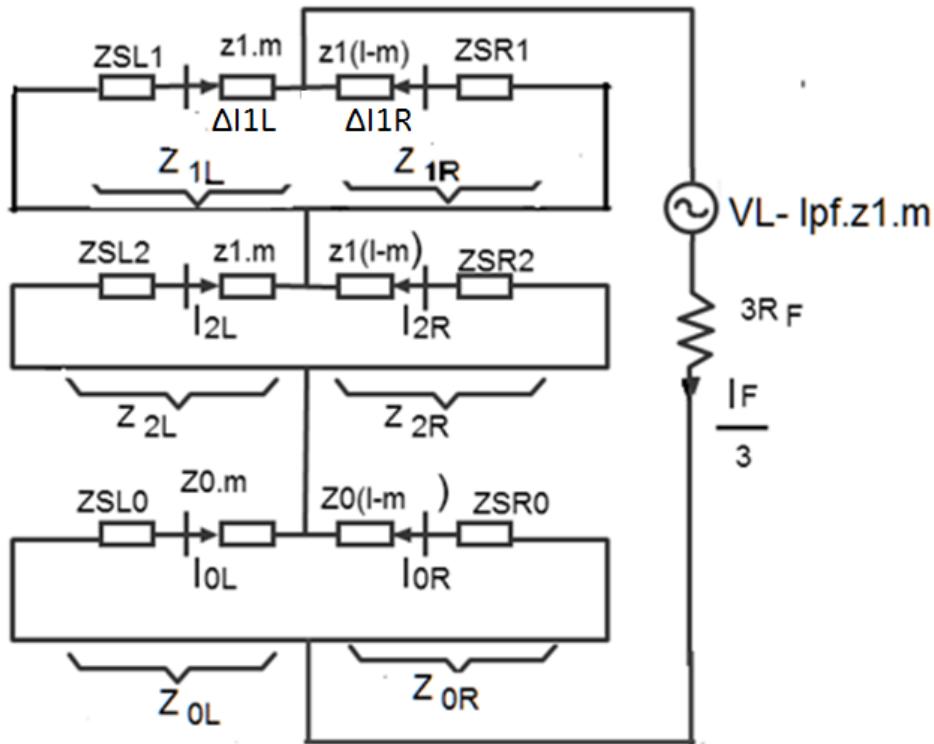


Figure 3: Superimposed Network Connection.

Where,  $Z_{total}$  is the total fault loop impedance;

$$Z_{total} = \frac{Z_{1L} \cdot Z_{1R}}{Z_{1L} + Z_{1R}} + \frac{Z_{2L} \cdot Z_{2R}}{Z_{2L} + Z_{2R}} + \frac{Z_{0L} \cdot Z_{0R}}{Z_{0L} + Z_{0R}} + 3R_F \quad (6)$$

Substituting (for the sake of convenience local relay on the left side is taken as reference and  $V_L$  is replaced by  $V$  and  $I_{pf}$  by  $I$ );

$$R_{app} = \left[ \frac{V - I \cdot z1 \cdot m}{Z_{total}} \right] \cdot \frac{3RF}{[I + (\Delta I1L + I2L + I0L) + k0 \cdot I0L]}$$

Now defining the Working Impedance (pre-fault impedance) as;

$$Z = V/I$$

substituting and simplifying;

$$R_{app} = \frac{3(Z - z1 \cdot m)RF}{\left\{ Z_{total} + (Z - z1m) \left[ \frac{Z1R}{Z1L + Z1R} + \frac{Z2R}{Z2L + Z2R} + \frac{Z0R}{Z0L + Z0R} (1 + k0) \right] \right\}} \quad (7)$$

From definition of k0;

$$1 + k0 = 1 + \frac{z0 - z1}{z1} = \frac{z0}{z1}$$

Substituting and simplifying;

$$R_{app} = \frac{3(Z - z1m)RF}{\left\{ 3RF + \frac{(Z + ZSL1) \cdot Z1R}{Z1L + Z1R} + \frac{(Z + ZSL2) \cdot Z2R}{Z2L + Z2R} + \frac{\left( Z \cdot \frac{z0}{z1} + ZSL0 \right) Z0R}{Z0L + Z0R} \right\}} \quad (8)$$

Defining c1, c2 and c0, sequence network current distribution factors as;

$$c1 = \frac{Z1R}{Z1L + Z1R} \quad (9)$$

$$c2 = \frac{Z2R}{Z2L + Z2R} \quad (10)$$

$$c0 = \frac{Z0R}{Z0L + Z0R} \quad (11)$$

$$R_{app} = \frac{3(Z - z1m)RF}{\left\{ 3RF + c1 \cdot (Z + ZSL1) + c2 \cdot (Z + ZSL2) + c0 \cdot \left( Z \cdot \frac{z0}{z1} + ZSL0 \right) \right\}} \quad (12)$$

Or, Rapp is obtained as;

$$R_{app} = \frac{3RF(Z - z1m)}{3RF + S} \quad (13)$$

Where;

$$S = c1(Z + ZSL1) + c2(Z + ZSL2) + c0 \left( Z \cdot \frac{z0}{z1} + ZSL0 \right) \quad (14)$$

S is a function of the circuit and fault parameters but is independent of the fault resistance RF.

The impedance measured by the relay;

$$Z_R = z_{1m} + R_{app}$$

$$Z_R = \frac{3R_F \cdot Z + z_{1m} \cdot S}{3R_F + S}$$

Rearranging;

$$\frac{Z_R - z_{1m}}{Z_R - Z} = -3R_F/S$$

Letting;

$$Y = -3/S$$

$$Y \cdot R_F = \frac{Z_R - z_{1m}}{Z_R - Z} \quad (15)$$

Here,  $R_F$  is the actual fault resistance, and has a real value,  $Z_R$  is the impedance measured by the distance relay during fault conditions and includes the line positive sequence impedance to the fault point ( $z_{1m}$ ) as well as the apparent fault resistance ( $R_{app}$ ) and,  $Z = V/I$  is the working impedance (prefault impedance measured by the relay).

From Equation 15 we can deduce;

For the phase angles;

$$\varphi = \text{Arg} \left\{ \frac{Z_R - z_{1m}}{Z_R - Z} \right\} = \text{Arg}\{Y\} \quad (16)$$

This equation defines an arc of a circle, the angle  $\varphi$  subtended by the chord ( $z_{1m} - Z$ ) as  $R_F$  is varied from zero to  $\infty$ , as shown in Figure 4.

And from the magnitudes;

$$R_F |Y| = \left| \frac{(Z_R - z_{1m})}{(Z_R - Z)} \right| \quad (17)$$

The value of actual fault resistance  $R_F$  can be calculated corresponding to the any value of apparent impedance measured by the relay.

The loci for  $Z_R$  are shown in Figure 5 for various values of  $\varphi$ , where the poles are denoted as L and K corresponding to  $z_{1m}$  and  $Z$ , respectively.

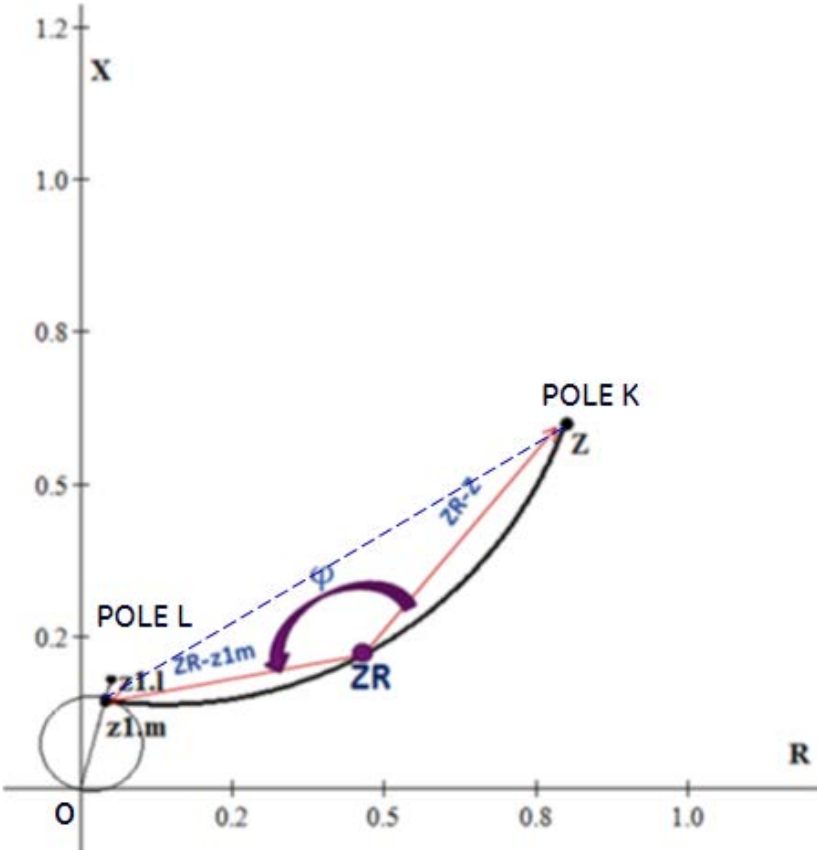


Figure 4: ZR, Impedance Measured by the Distance Relay.

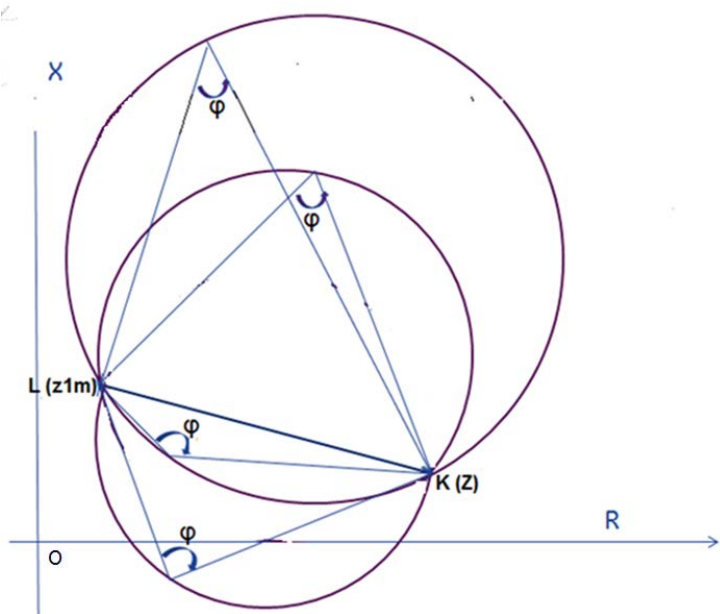


Figure 5: Loci of ZR for Various Values of φ

### 2.3 Calculation of center coordinates and radii

From Figure 6, the center point is obtained as;

$$M = z1.m + r \angle (\varphi - 90^\circ) + \text{Arg} (Z - z1.m) \quad (18)$$

Substituting from figure 6;

$$\cos (\varphi - 90) = \sin \varphi = |LK| / 2r$$

Therefore then radius r is obtained as;

$$r = \frac{|LK|}{2 \cdot \sin \varphi} \quad (19)$$

and the center coordinates as;

$$OM = z1.m + |LK| / 2 \sin \varphi \angle \varphi - 90^\circ + \text{Arg} LK$$

$$OM = z1.m + LK \cdot (1/2 \sin \varphi) \angle \varphi - 90^\circ$$

Or simplifying;

$$OM = z1.m + [1 - j \cot \varphi] \cdot \frac{LK}{2} \quad (20)$$

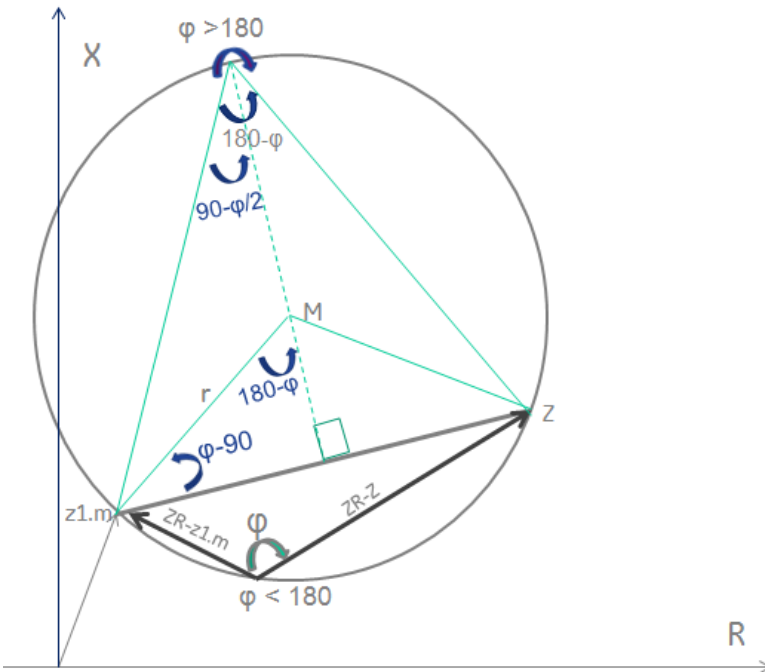


Figure 6: Calculation of Center Coordinate and Radii.



## 2.4 Calculation of measured impedance corresponding to an actual fault resistance (RF) value

Equation 17 is repeated below;

$$Y. RF = \frac{ZR - z1.m}{ZR - Z}$$

From Figure 7, writing the cosine law for triangle (ZR-M-K);

$$|KZR|^2 = 2r^2 - 2r^2 \cos 2\alpha$$

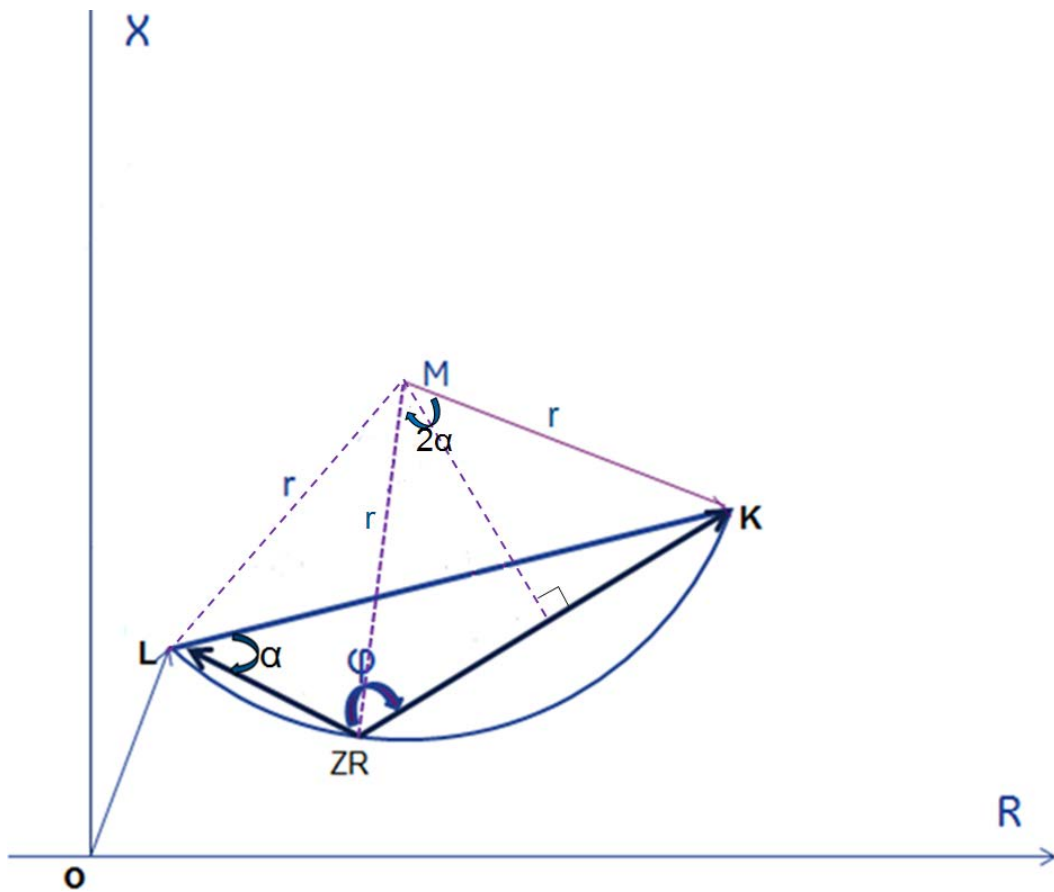


Figure7: Calculation of Relay Measurement ZR Corresponding to a Given Fault Resistance RF.

From Figure 7, writing the cosine law for triangle (ZR-M-K);

$$|KZR|^2 = 2r^2 - 2r^2 \cos 2\alpha$$

$$|KZR|^2 = 2r^2 (1 - \cos 2\alpha) = 4r^2 \cdot \sin^2 \alpha$$

Hence;

$$\sin \alpha = |KZR|/2r \quad (21)$$

Defining n as;

$$n = \frac{|LZR|}{|KZR|} = RF|Y| \quad (22)$$

$$\sin \alpha = |LZR|/2r \cdot n$$

Now writing cosine law for triangle (L-ZR-K)

$$|LK|^2 = |LZR|^2 + |KZR|^2 - 2 \cdot |LZR| \cdot |KZR| \cdot \cos \varphi$$

$$|KZR| = \frac{|LK|}{\sqrt{(n^2 - 2n \cos \varphi + 1)}} \quad (23)$$

As we know the value of ZR and the locus parameters |LK| and n are also known, |KZR| and |LZR| can be calculated.

Therefore the apparent resistance can be written as;

$$R_{app} = |LZR| \angle (\arg LK - \alpha) \quad (24)$$

The apparent resistance measurement,  $R_{app} = LZR$ , for a given actual resistance value, RF, can be calculated similarly from known parameters.

## 2.5 Calculation of relay reaches

The relay reach is defined as the limit point of relay operation where the impedance measured by the relay falls on the relay threshold characteristic.

Therefore, the relay reach is calculated as the intersection point(s) of loci with the relay operation characteristics or its components (e.g. blinder and inductive settings in a quad relay or for a mho relay circular operating characteristic). Intersection points are calculated simply by finding the common solutions for the respective curves.

Once the points of intersection are calculated it is very simple to find the corresponding **actual resistive reach** of the relay using Equation 22 above.

### 3. Special cases

#### 3.1 Local end feed only

In this case the remote terminal is assumed to be open circuit.

Fault condition is shown in the following Figure 8;

Where;

$$I_1 = I_2 = I_0 = \frac{I_F}{3} = \frac{E}{Z_{1L} + Z_{2L} + Z_{0L} + 3R_F}$$

And the impedance measured by the relay;

$$Z_R = \frac{V}{I_A + k_0 I_0} = z_{1m} + \frac{I_F R_F}{I_A + k_0 I_0}$$

$$Z_R = z_{1m} + \frac{3R_F}{3 + k_0} \quad (25)$$

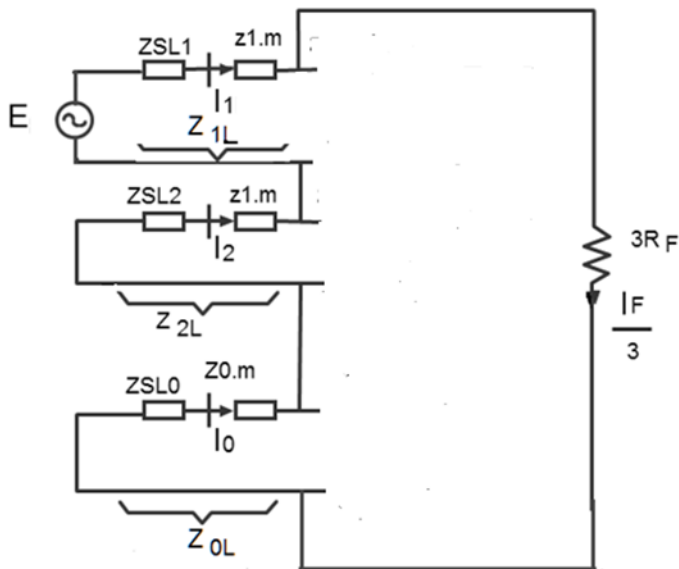


Figure 8: Phase to Ground Fault with Single End Feed Conditions.

The apparent fault resistance;

$$R_{app} = \frac{3R_F}{3 + k_0}$$

is independent of the position of fault on the protected line.

For a line with;

Line positive sequence impedance ( $z_1$ ) = 0.025+j0.6 ohms/mile

Line zero seq. impedance ( $z_0$ ) = 0.3+j1.8 ohms/mile

$$k_0 = (z_0 - z_1)/z_1 = 2.05 \angle -10.5^\circ$$

$$R_{app} = 0.596R_F \angle 4.3^\circ$$

The relay will measure about 60% of the fault resistance and therefore the resistive reach of the relay is considerably extended along the resistive axis (about 67% for a reactance relay) with a small overreach or underreach (depending on the angle of  $R_{app}$ ) along the reactance axis, as shown in Figure 9.

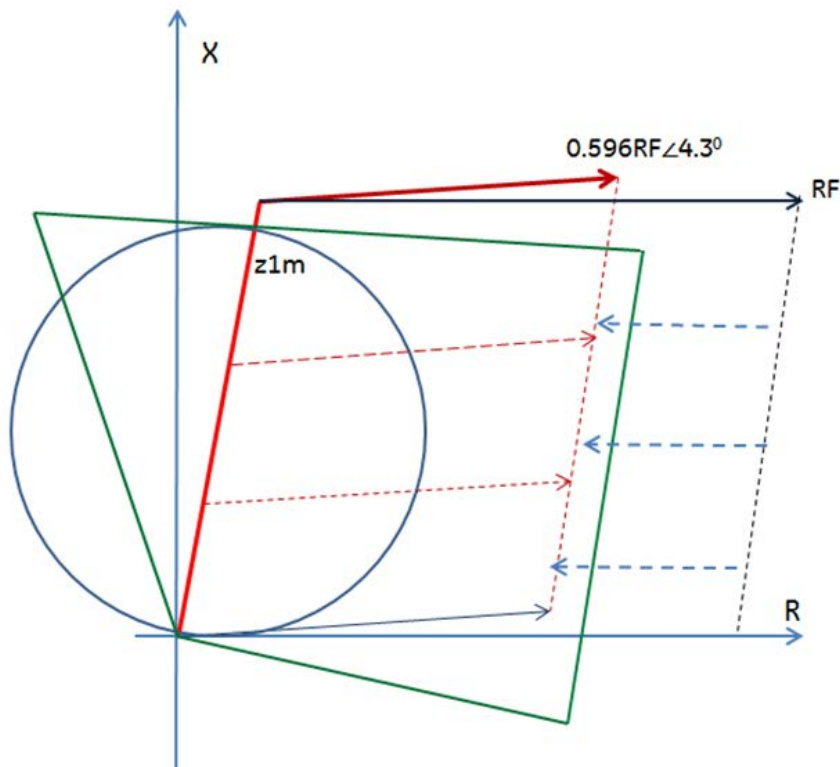


Figure 9: Single End Feed and Fault Resistance Measurement.

### 3.2 Prefault Current =0, Z=∞

Substituting ∞ for the value of Z in Equation 12 repeated below;

$$R_{app} = \frac{3(Z - z_{1m})RF}{\{3RF + c_1.(Z + Z_{SL1}) + c_2.(Z + Z_{SL2}) + c_0.\left(Z.\frac{z_0}{z_1} + Z_{SL0}\right)\}}$$

$$R_{app} = \frac{3RF}{\left[c_1 + c_2 + c_0\left(\frac{z_0}{z_1}\right)\right]} \quad (26)$$

As defined in Section 2.2 c<sub>1</sub>, c<sub>2</sub> and c<sub>0</sub> are current distribution factors in the positive, negative and zero sequence networks and depend on the values of circuit impedances as well as the location of the fault, and their magnitudes are always smaller than unity. However, z<sub>0</sub>/z<sub>1</sub> value is about 2-3 for most of the transmission lines, therefore, depending on the location of the fault and system parameters the relay may overreach or underreach during phase to ground faults .It is clear that the locus will be a straight line starting at z<sub>1m</sub>.

It is noted that depending on the homogeneity of the system parameters, the relay will be measuring some amount of reactance ( capacitive or inductive ), the term homogeneity refers to current distribution factors c<sub>1</sub>,c<sub>2</sub> and c<sub>0</sub> all having real values, or practically all system impedances of same phase angle value. The locus is shown in Figure 10 for the sample system shown in Figure 11, with equal sources of j25 Ω on each end and for various fault locations (inductive components were very small and only vector magnitudes were shown).

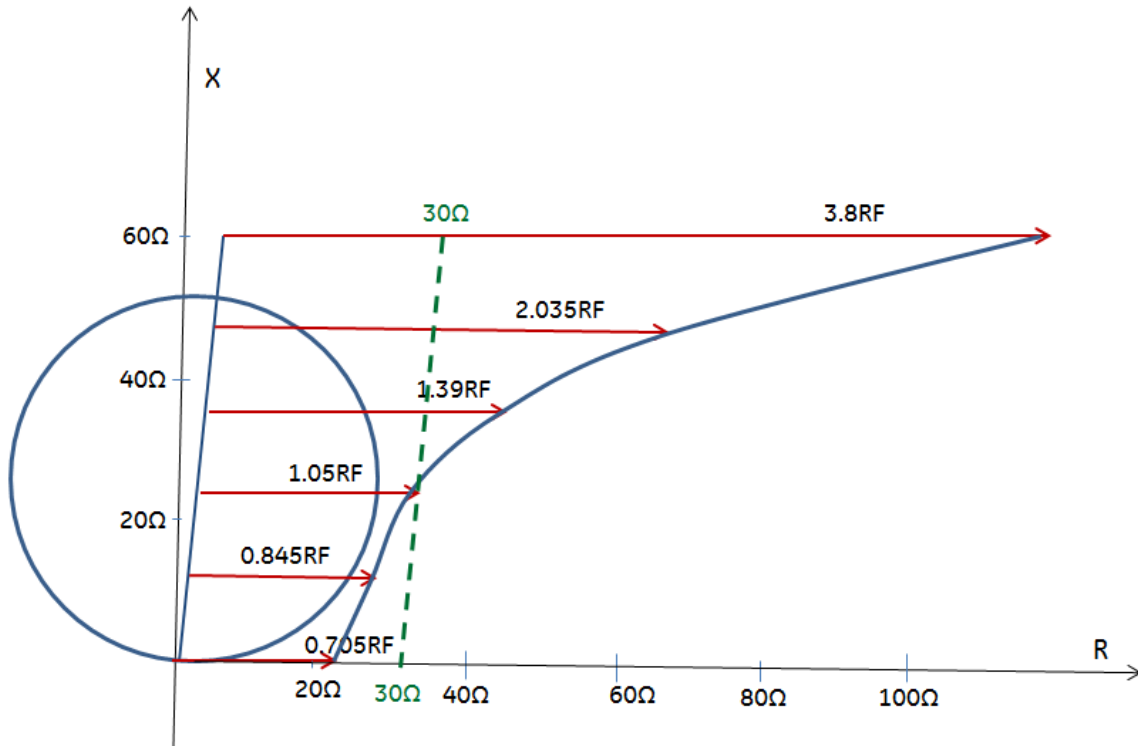
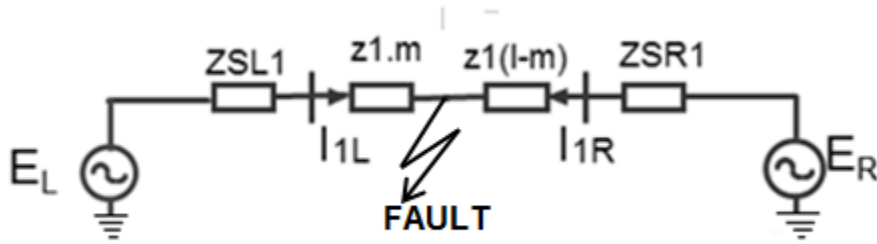


Figure 10: Fault Locus with RF= 30Ω, Z=∞, Equal Source Impedances.



$$E_L = 500/\sqrt{3} \text{ kV} \angle \delta$$

$$Z_{SL1} = Z_{SL2} = Z_{SL0} = j25 \text{ } \Omega$$

$$E_R = 500/\sqrt{3} \text{ kV} \angle 0^\circ$$

$$Z_{SR1} = Z_{SR2} = Z_{SR0} = j25 \text{ } \Omega$$

Line length = 100 miles  
 Line positive seq. imp. ( $z_1$ ) = 0.025 + j0.6  $\Omega$ /mile  
 Line zero seq. imp. ( $z_0$ ) = 0.3 + j1.8  $\Omega$ /mile

Figure 11: Sample Power System

#### 4. The Working Impedance

The working impedance is defined as the impedance measured by the relay in the power system shown in Figure 12 just before the occurrence of the fault and is defined as;

$$Z = V/I$$

Where, V and I are the relay voltage and current.

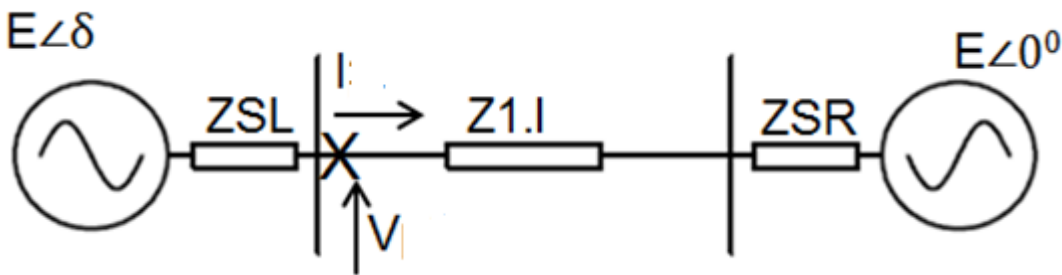


Figure 12 Power System before the occurrence of fault.

The term "Working impedance" was first used by J. Zydanowicz (Ref.1) and we decided to keep it. The load current or pre-fault current may be calculated as;

$$I = \frac{E_L \angle \delta - E_R \angle 0^\circ}{Z_{SL} + Z_{SR} + z_{1l}}$$

Or;

$$I = \frac{E\angle\delta - E\angle 0}{ZT}$$

Referring to Reference 2 ,and considering that, the conditions and calculations made for power swings are equally applicable to pre-fault conditions corresponding to an instance of the power system before the fault ,we can express the current as;

$$I = \left(2 \cdot \frac{E}{ZT}\right) \cdot \sin\left(\frac{\delta}{2}\right) \angle \left(90 + \frac{\delta}{2}\right) \quad (27)$$

And the working impedance Z;

$$Z = \frac{V}{I} = \left(\frac{ZT}{2}\right) \left[1 - j\cot\left(\frac{\delta}{2}\right)\right] - ZSL \quad (28)$$

The geometrical interpretation of the Equation 28 is represented in Figure 13. The trajectory of the measured impedance at the relay during pre-fault or load condition , as well as a power swing condition corresponds to a straight line that intersects the segment A to B at its middle point, as the angle  $\delta$  between the sources varies. This point is called the **Electrical Center** of the swing. The angle between the two segments that connect K to the two source points is equal to  $\delta$  as shown in Figure 13. When the angle  $\delta$  reaches the value of  $180^\circ$ , the relay impedance is precisely at the location of the electrical center. It can be seen that the impedance trajectory during an unstable power swing will cross any relay operating characteristic that covers the line, provided that the electrical center falls inside the zone covered by the relay.

It is also assumed that any pre-fault operating condition of the power system can be considered as an instant of a power swing, swinging usually at frequencies below 4-5 Hz, or; a swing condition can be considered as a continuous succession of pre-fault load conditions. Therefore, the fault calculations covered in this paper are equally applicable to all pre-fault conditions, may they correspond to a load or a power swing. Depending on value of  $\delta$  our pole K will move along the “**Swing Line**” and hence define the loci of impedances seen by our distance relay, ZR, along with the other pole L corresponding to the point of fault on the protected line (z1m).

The working impedance for the remote end can be calculated as;

$$Z' = [V_{pf} - I_{pf} \cdot z1] / -I$$

Or,

$$Z' = -Z + z1 \cdot I \quad (29)$$

The active power expression for the relay terminal (Ref 2) is;

$$P = V^2 \frac{\sin\delta}{X_{line}} \quad (30)$$

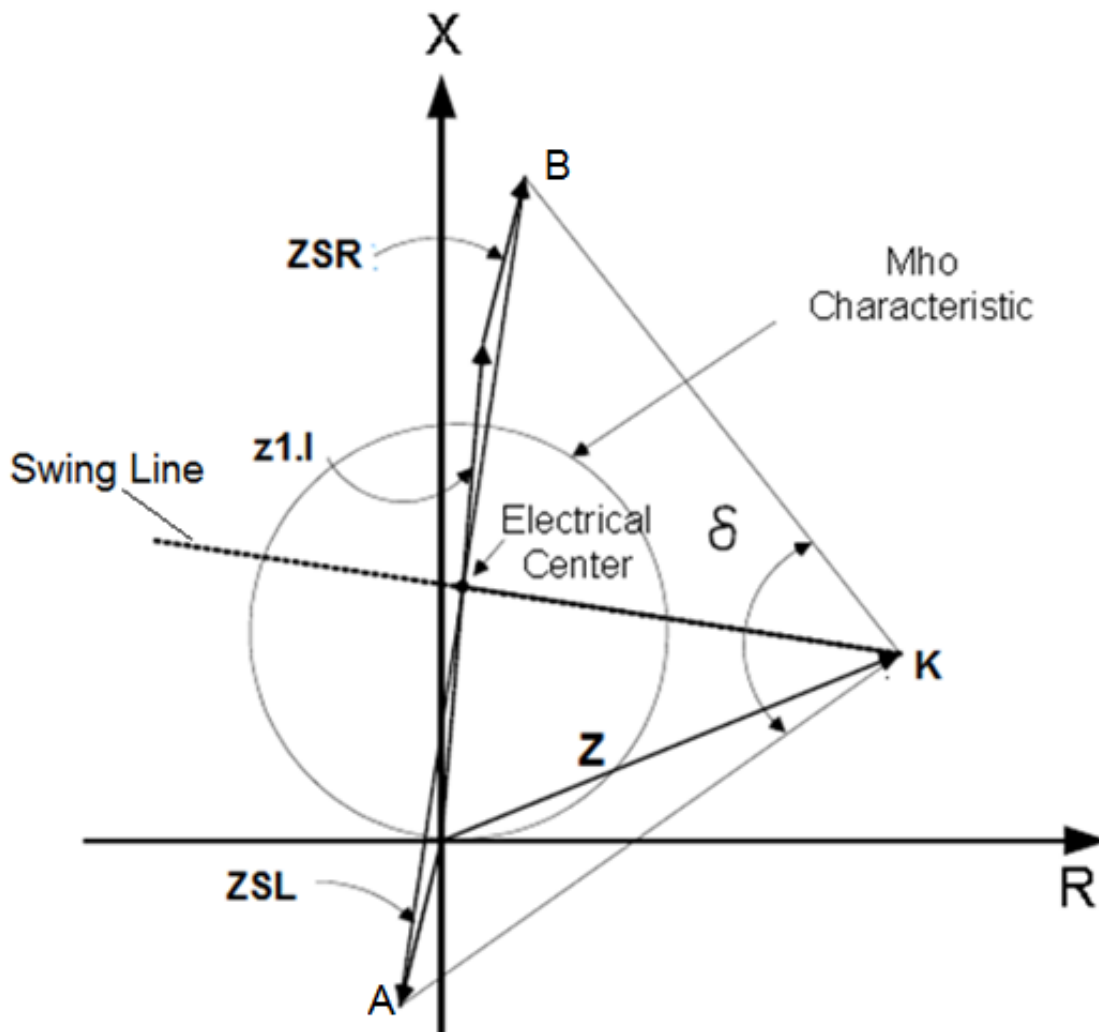


Figure 13: Calculation of Z, the Working Impedance.

We can conclude that the sign of  $\sin\delta$ , or the sign of  $\delta$ , defines the direction of power flow, and positive values of  $\delta$  represents **Power Exported** at the relay terminal, while for the negative values **Power is Imported**.

Working impedance values and the trajectory of K pole (swing line) are shown in Figures 14 and 15 for equal and weak source conditions, respectively, for different values of  $\delta$ .



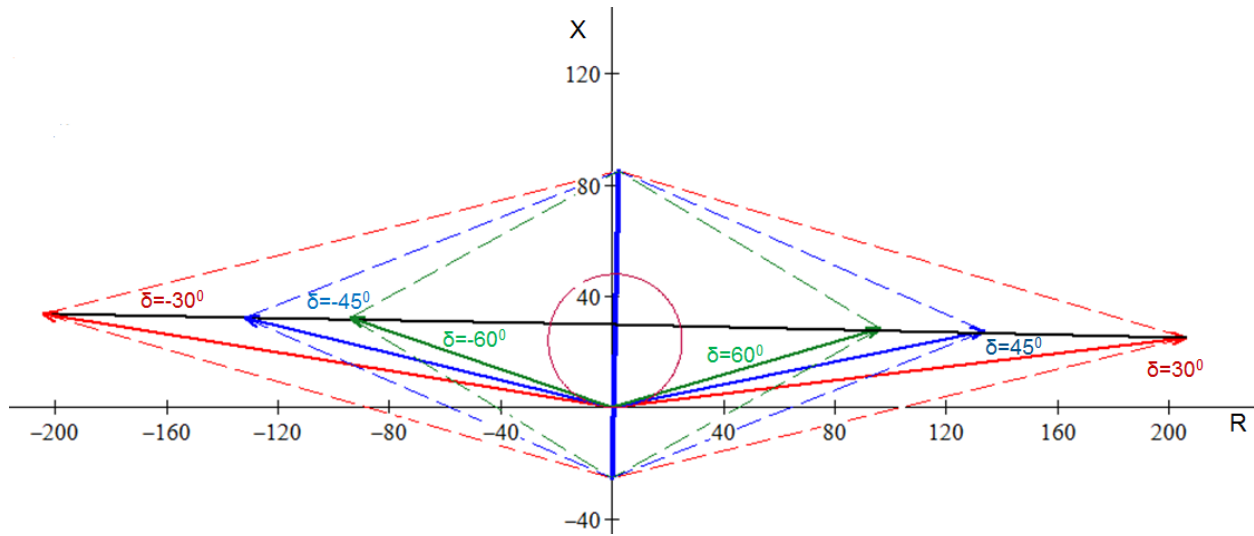


Figure 14: Working impedance, Z, Values for the Sample system (equal Sources of j25 ohms).

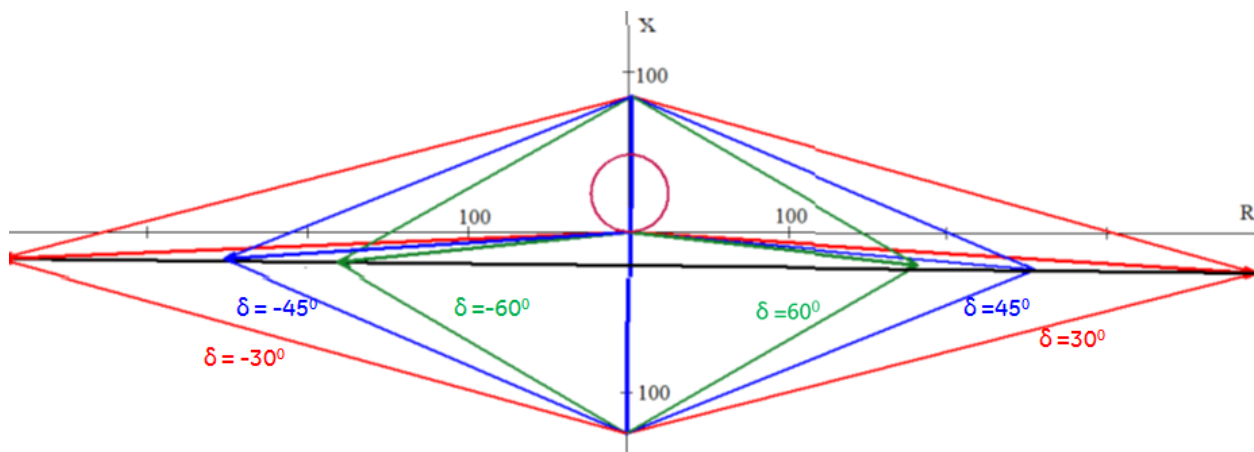


Figure 15: Working Impedance, Z, Values for the Sample System (Weak Local Source of j125 ohms).

## 5. Display of ZR loci and other pre-fault and fault parameters on the Impedance plane

A summary of the impedances seen by the distance relay under pre-fault and fault conditions and the relations between them is displayed in the impedance plane in Figure 16 and 17. The figures also cater for the dynamic expansion of the mho operating characteristics with memory or cross-polarized distance relays, where the operating zone is extended in the source direction by an impedance equal to the source impedance and mho circle center location and diameter are augmented accordingly.

Figure 17 shows the additional impedances measured by the relay  $\Delta R$  and  $\Delta X$ , these may also be considered as measurement errors due to fault resistance  $R_F$  and pre-fault power flow.

When the measured impedance,  $Z_R$ , is on the relay operating characteristic as shown in Figure 17, then the corresponding value of the actual fault resistance,  $R_F$ , defines the **reach** of the relay, the relay is said to **underreach** along resistance,  $R$ , or reactance,  $X$ , axis when corresponding  $\Delta R$  and/or  $\Delta X$  value is positive (**inductive for  $\Delta X$** ) with reference to  $R_F$  (Figure 17a), and the area of operation is reduced. When the values of  $\Delta R$  and/or  $\Delta X$  are negative (**capacitive for  $\Delta X$** ) then the relay **overreaches**. In some cases values of  $\Delta R$  or  $\Delta X$  may have different polarities with respect to  $R_F$ , in such cases the underreach or overreach applies to the corresponding axis,  $R$  or  $X$ , e.g. and relay may underreach along  $R$  axis but overreach along  $X$  axis as shown in Figure 17b. It is noted that underreach or overreach  $\Delta R$ , refers to the fault resistive coverage of the relay only, and the analysis is only valid for phase to ground fault conditions and does not apply to load conditions (e.g. does not apply to encroachment). However,  $\Delta X$  depending on the polarity causes overreach and underreach along the protected line and defines the security and coverage of the relay, respectively.

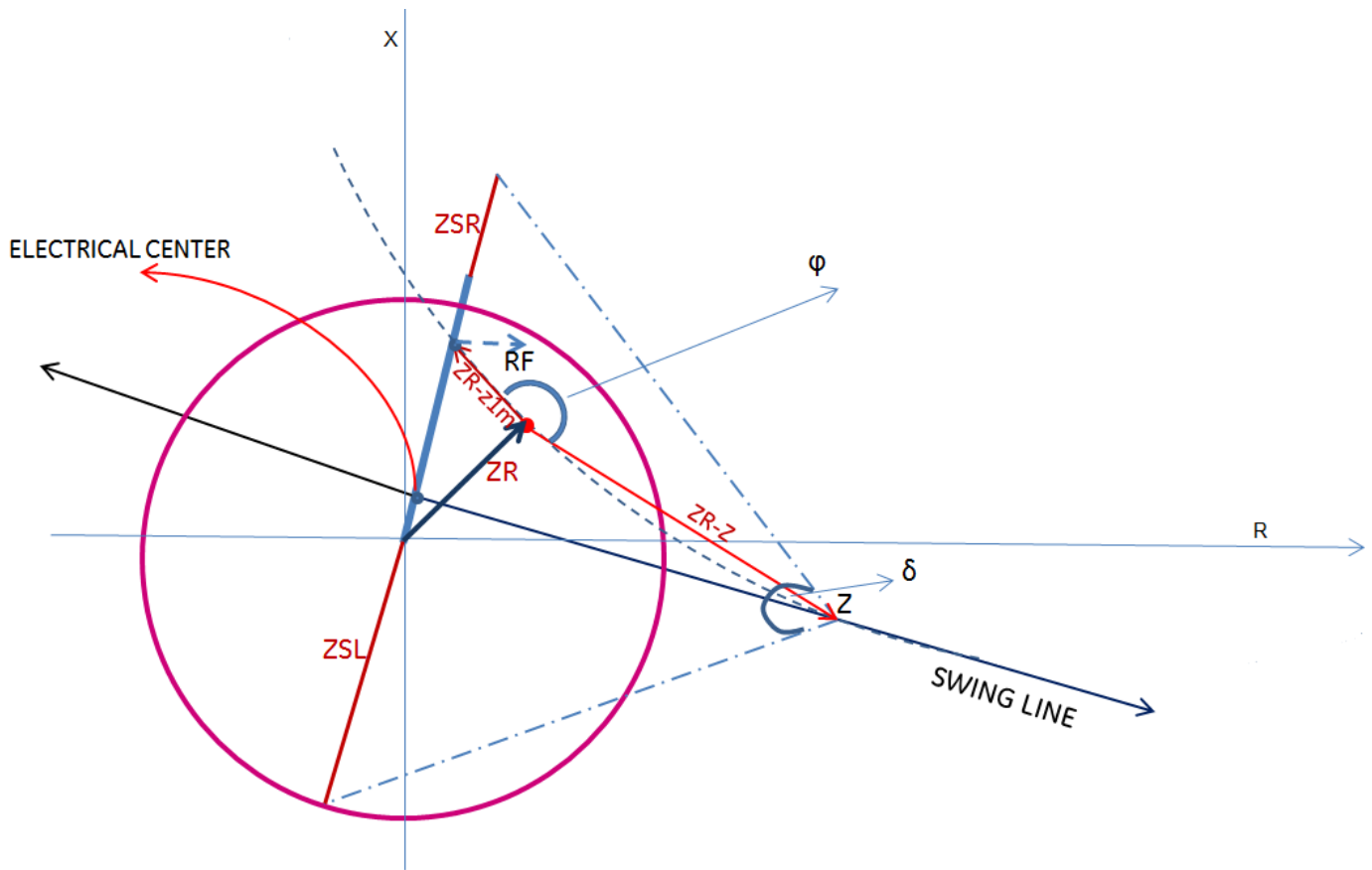


Figure 16: Impedances Seen by the Distance Relay.

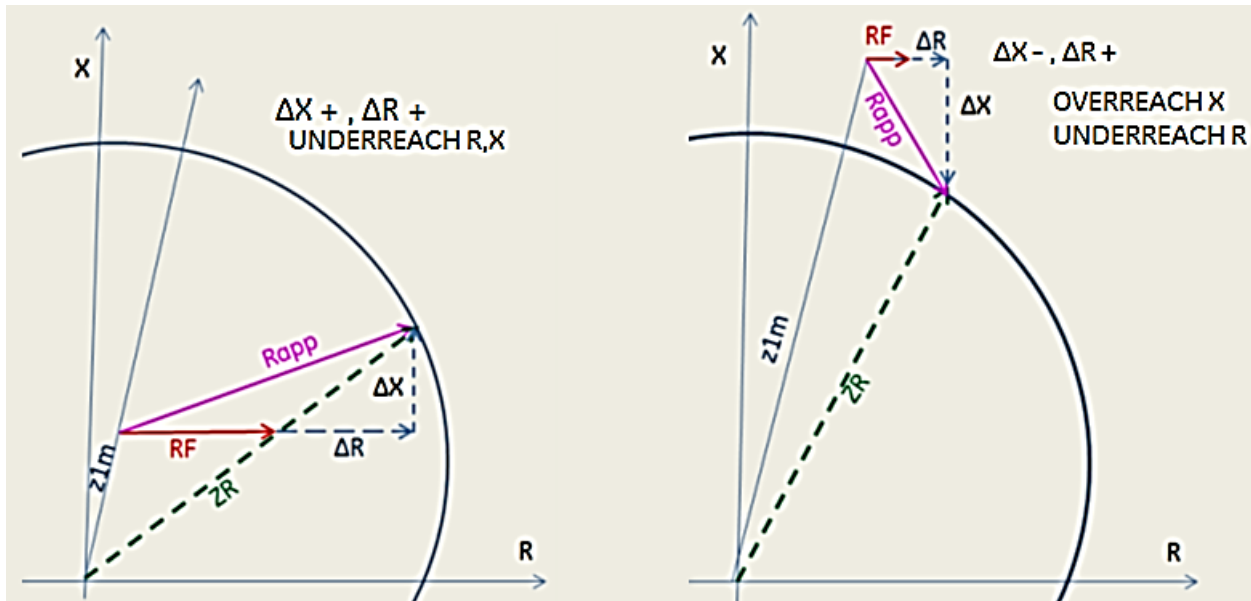


Figure17: Apparent and Actual Fault Resistances

(a) Underreach in R and X

(b) Overreach in X, underreach in R

The loci of  $Z_R$  impedances are shown for both pre-fault power export ( $\delta=30^\circ$ ) and import ( $\delta=-30^\circ$ ) as well as equal and weak source conditions in Figures 18 and 19, respectively. Impedances measured for fault resistances of 10, 20, 30, 50, 100 $\Omega$  and  $\infty$  are shown on the figures.

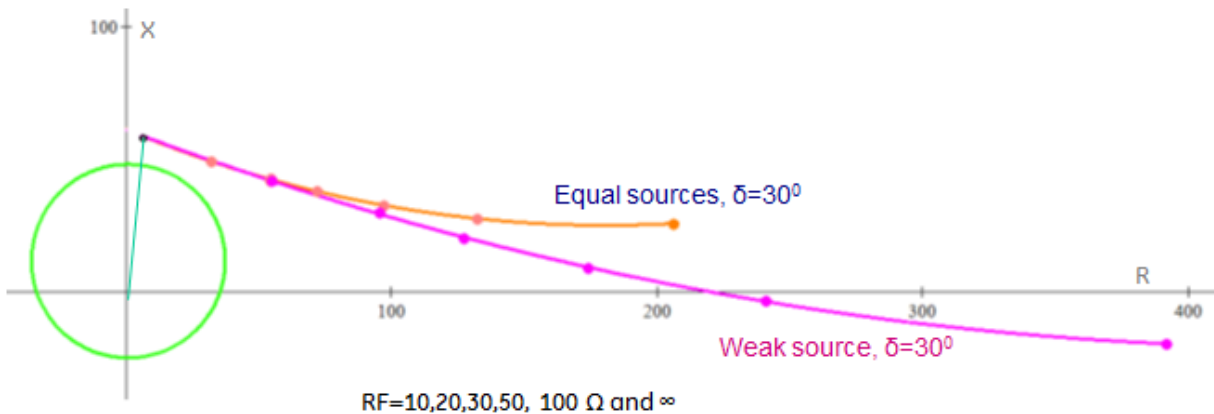


Figure 18:  $Z_R$  Loci for Power Export,  $\delta=30^\circ$ , for Both Equal and Weak Source Conditions, Fault at the Remote Terminal,  $m=100\%$ .

From Figure 18 it can be seen that under pre-fault power export conditions the apparent fault resistance as measured by the relay has a negative  $\Delta X$  (capacitive reactance) component and the resistive component is larger than the actual fault resistance ( $\Delta R$ , positive). Hence, relays set with reference to

the protected line's inductive reactance would tend to overreach along the X axis and underreach along the R axis.

The method of analysis and calculations are valid for internal faults only, for faults beyond the remote terminal the protected line becomes a part of the local source impedance, hence possible misoperation of relays for faults on adjacent line(s) has not been a subject of this paper. Nevertheless, for close faults on the adjacent lines the operating conditions for the local relay are quite similar to the case with remote terminal faults and the relay may overreach and misoperate. For such cases the remote end relay would be exposed to a reverse fault condition and would not misoperate. The amount of reactance overreach and resistive underreach is more serious for weak source conditions..

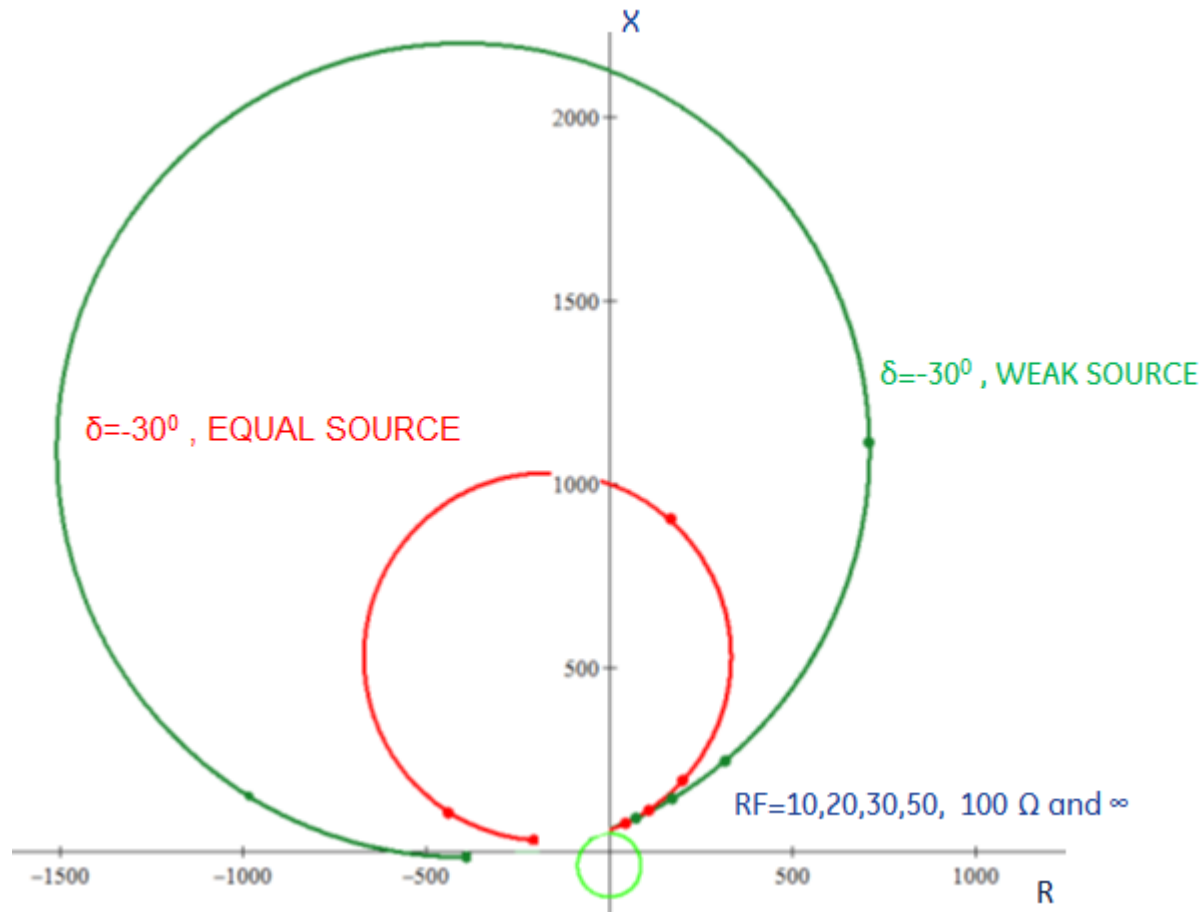


Figure 19: ZR Loci for Power Import,  $\delta=-30^\circ$  for Both Equal and Weak Source Conditions, Fault at the Remote Terminal,  $m=100\%$ .

Similarly, for the pre-fault power import case (Figure 19) the apparent fault resistance has an inductive reactance component,  $\Delta X$  positive, and also the resistive part of the measurement is larger than the actual fault resistance, i.e.  $\Delta R$  is positive. Hence, relays set with reference to the protected line's inductive reactance would underreach and have reduced coverage along both R and X axis. The amount of underreach is more serious for weak source conditions, relays set to about 80% would seriously underreach and may not even cover 50% of the line depending on the amount of remote end infeed. The impedances measured by relays and relay reaches are studied in greater details in the following sections

## 6. Equal Sources at both terminals

First loci study is performed on the sample system shown in Figure 11 assuming equal source at both ends. In this case electrical center is in the middle point of the line. Studies are made for swing angle  $\delta$ , values of  $30^\circ$ ,  $60^\circ$ , and  $-60^\circ$  and displayed in Figure 20, the relay measurements corresponding to certain values of actual fault resistance are also shown. Different fault locations are selected 0, 20, 40, 80 and 100% of line length.

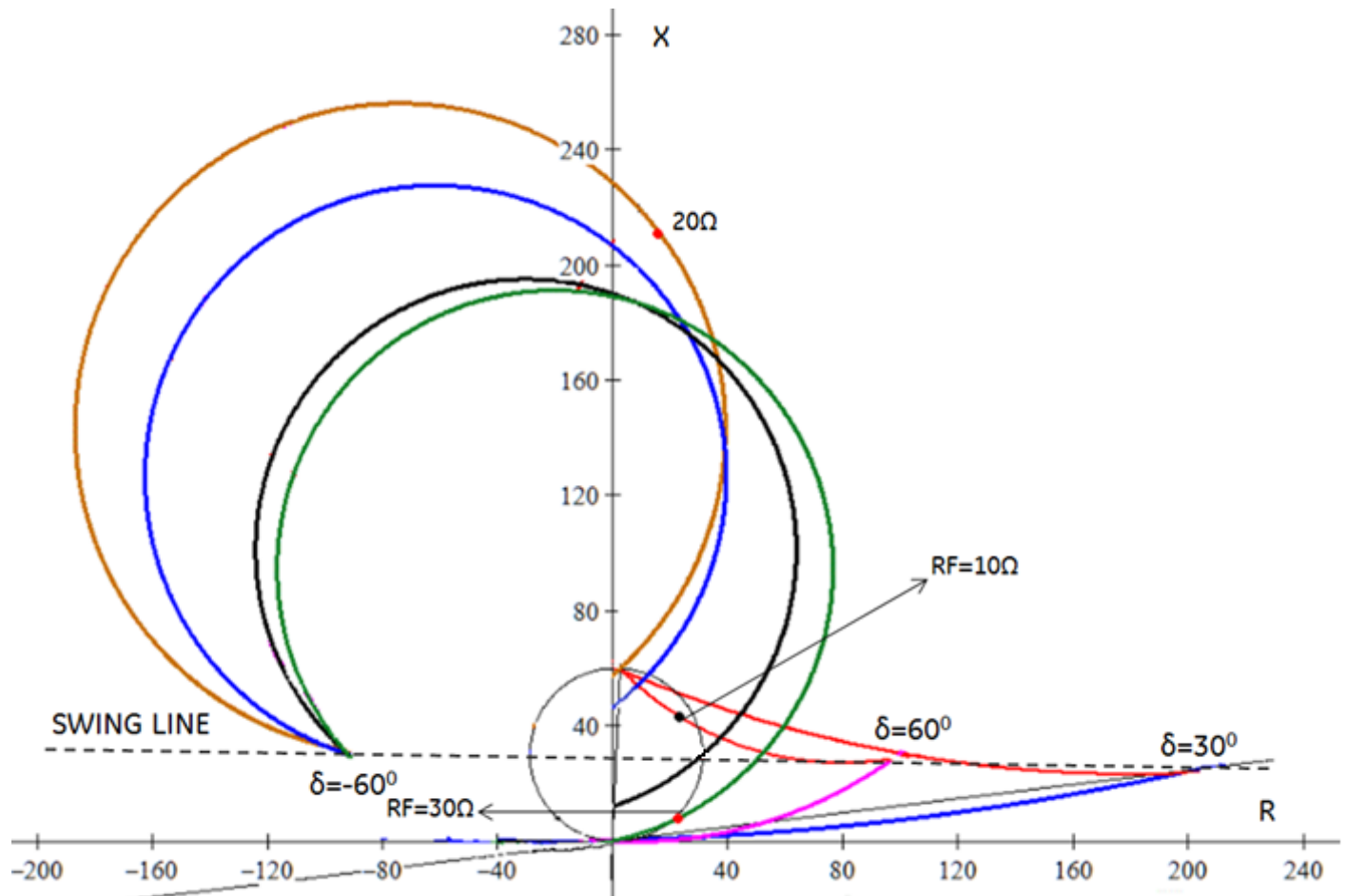


Figure 20: Impedance Loci for Equal Source Conditions, Different Swing Angle and Fault Locations.

Actual resistive reaches are calculated with  $\delta=30^\circ$  for an assumed typical mho characteristic, dynamic expansion of  $ZS=j25\Omega$  is also applied to the mho circle as shown in Figure 21.

It is noted that with the swing line passing through the line mid-point, K poles of the loci are approximately on the vertical line from the electrical center and this results in a minimum of over or underreach for the relays. As expected for about first 50% of the line the relay overreaches along the R axis ( $\Delta R$  negative) but for the remaining underreaches, the actual resistive reach values are points of

intersection of the loci with the mho relay, similarly, the relay slightly underreaches for the first 50% and overreaches for the rest of the fault locations along the X axis.

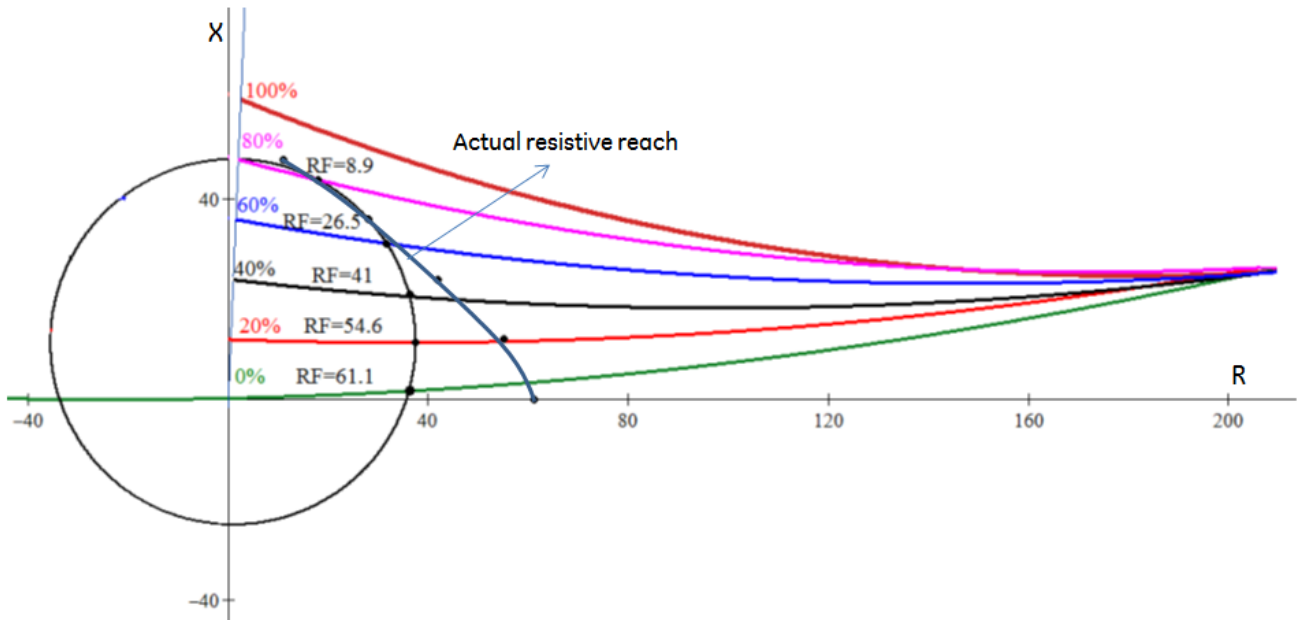


Figure 21: Actual Resistive Reaches, Equal Sources, Power Exported,  $\delta=30^\circ$

Reach calculations are repeated for power import cases with  $\delta=-30^\circ$  and results are displayed in Figure 22 for fault locations varied at 20% steps.

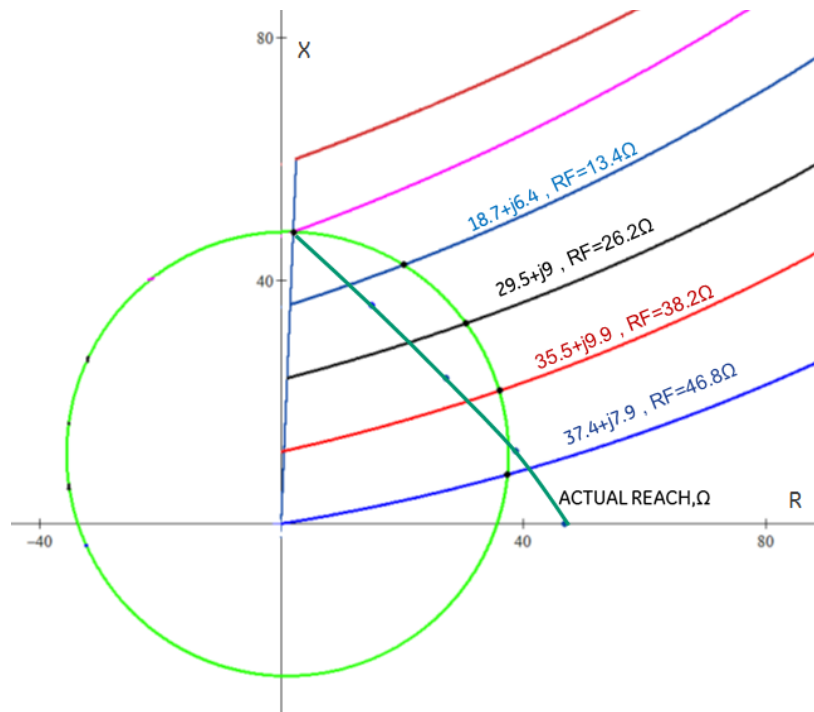


Figure 22 Actual Resistive Reaches, Equal Sources, Power Imported,  $\delta=-30^\circ$

As seen from the figure an actual fault resistance of  $R_F=46.8\Omega$  for a fault at relay location, i.e.  $m=0$ , is measured as  $37.4+j7.9\Omega$  and displays an overreach of about  $\Delta R=37.4-46.8=-9.4\Omega$  along the R axis and an underreach of  $\Delta X=j7.9\Omega$  along the X axis. As the fault location is moved along the line the amount of underreach increases, for example, for a fault at  $m=60\%$  the actual reach is  $13.4\Omega$  but is measured as  $18.7+j6.4\Omega$ . Other values are shown in Figure 22.

As a final analysis for the equal source case, a swing angle of  $\delta=-60^\circ$  is employed, the loci are shown in Figure 23 for varying fault locations from the line terminal in steps of 20%.

Figure 24 displays the corresponding resistive reaches for each fault location assuming an expanded mho characteristic. Comparing Figure 22 and 24 it can be seen that as the swing angle increases in the import direction, both resistive and inductive components of the apparent fault resistance are affected. As seen from the figure an actual fault resistance of  $R_F=46.3\Omega$  for a fault at relay location, i.e.  $m=0$ , is measured as  $37.2+j16.5\Omega$  and corresponds to an overreach of  $\Delta R=37.2-46.3=-9.1\Omega$  and an underreach of  $\Delta X=j16.5\Omega$ . As the fault location is moved along the line the amount of underreach increases, for example, for a fault at  $m=60\%$  the actual resistive reach is  $24.1\Omega$  but is measured as  $23+j16.1\Omega$ . Other values are shown in Figure 24. At this higher value of the swing angle underreach conditions are more severe.

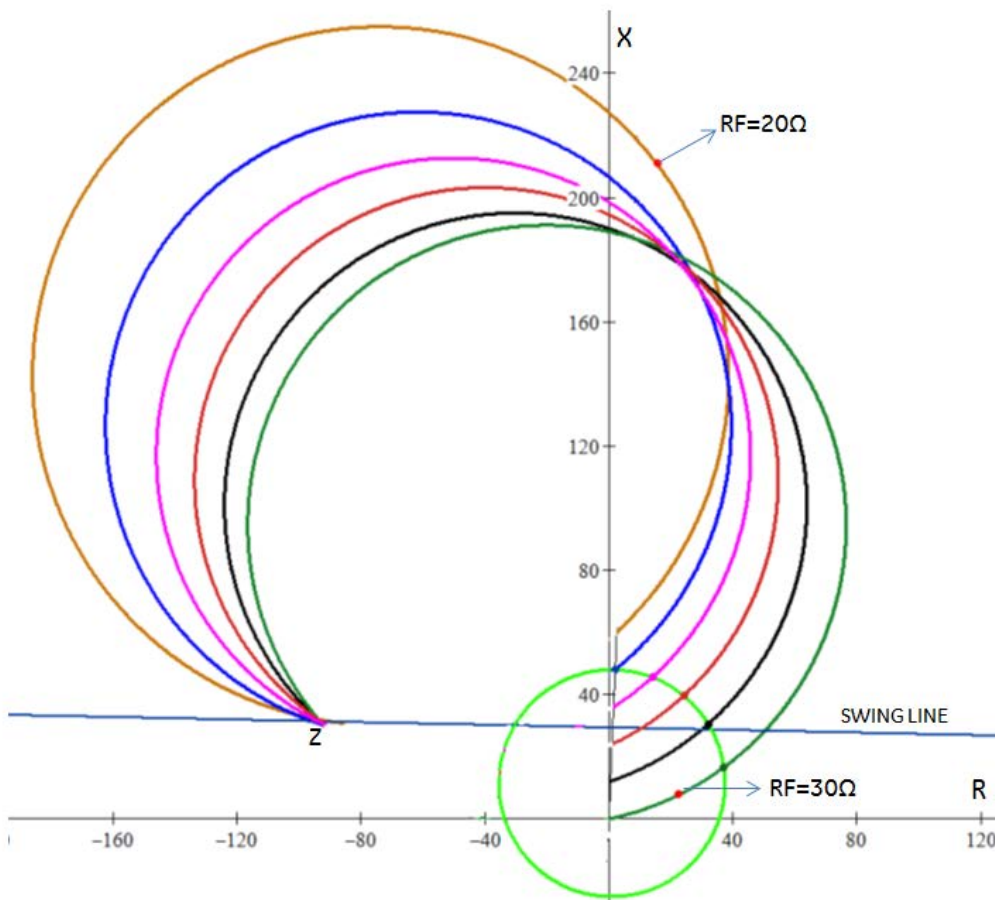


Figure 23: Impedance Loci for Equal Source Conditions, Power Imported,  $\delta=-60^\circ$ ,  $Z=-94.3+j31.7\Omega$ , and Different Fault Locations.

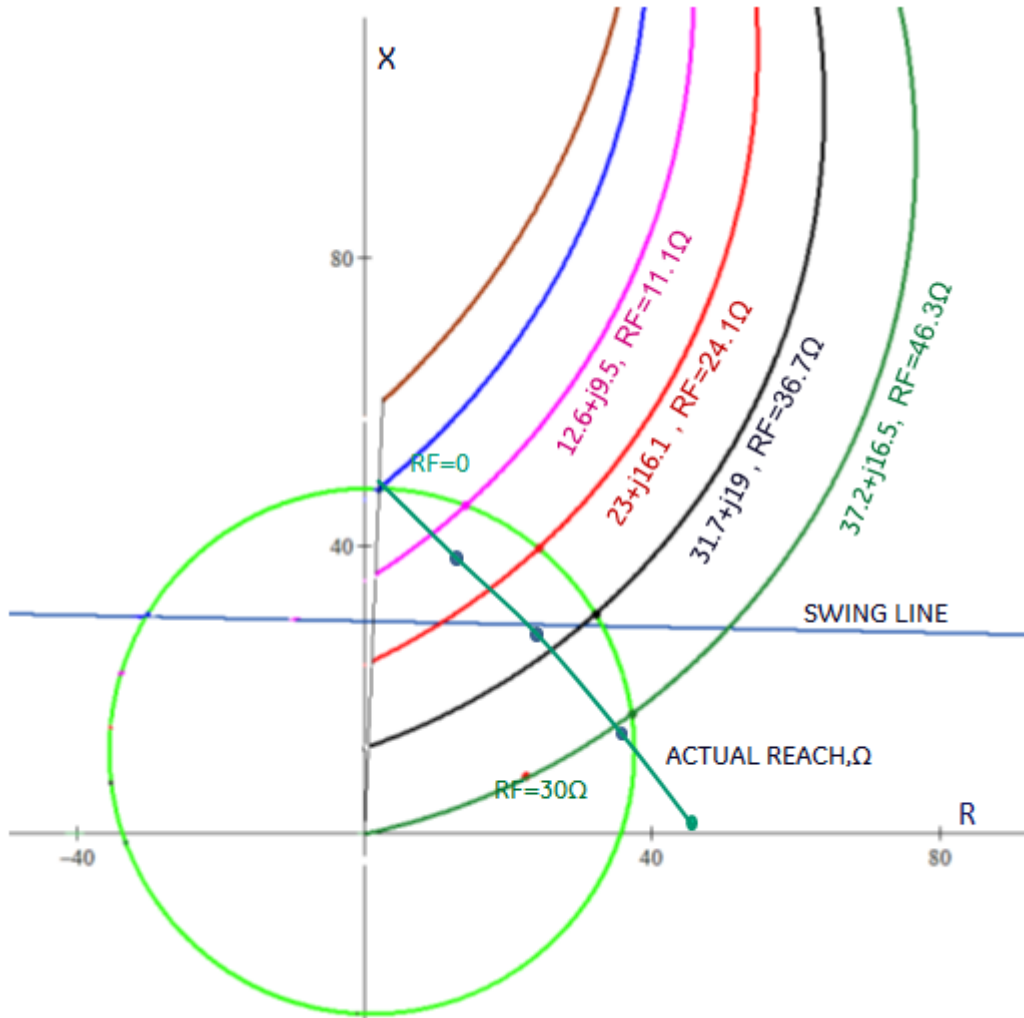


Figure 24: Actual Resistive Reaches, Equal Sources, Power Imported,  $\delta = -60^\circ$

## 7. Weak Source at the local terminal

This loci study is performed on the sample system shown in Figure 11 assuming a source impedance of  $j125\Omega$  at local and  $j25\Omega$  source at the remote end. In this case electrical center is in the behind the relay location.

### 7.1 Power exported at the local terminal

First the studies are made for swing angle  $\delta$  values of  $15^\circ$ ,  $30^\circ$  and  $60^\circ$  (pre-fault power export) and for faults at terminals. The results are displayed in Figure 25.

Actual resistive reaches are calculated for an assumed typical mho characteristic (with dynamic expansion corresponding to  $ZS = j125\Omega$ ) as well as an assumed quad characteristics set to cover 80% of the line for each terminal faults (Figure 26 and Figure 27).



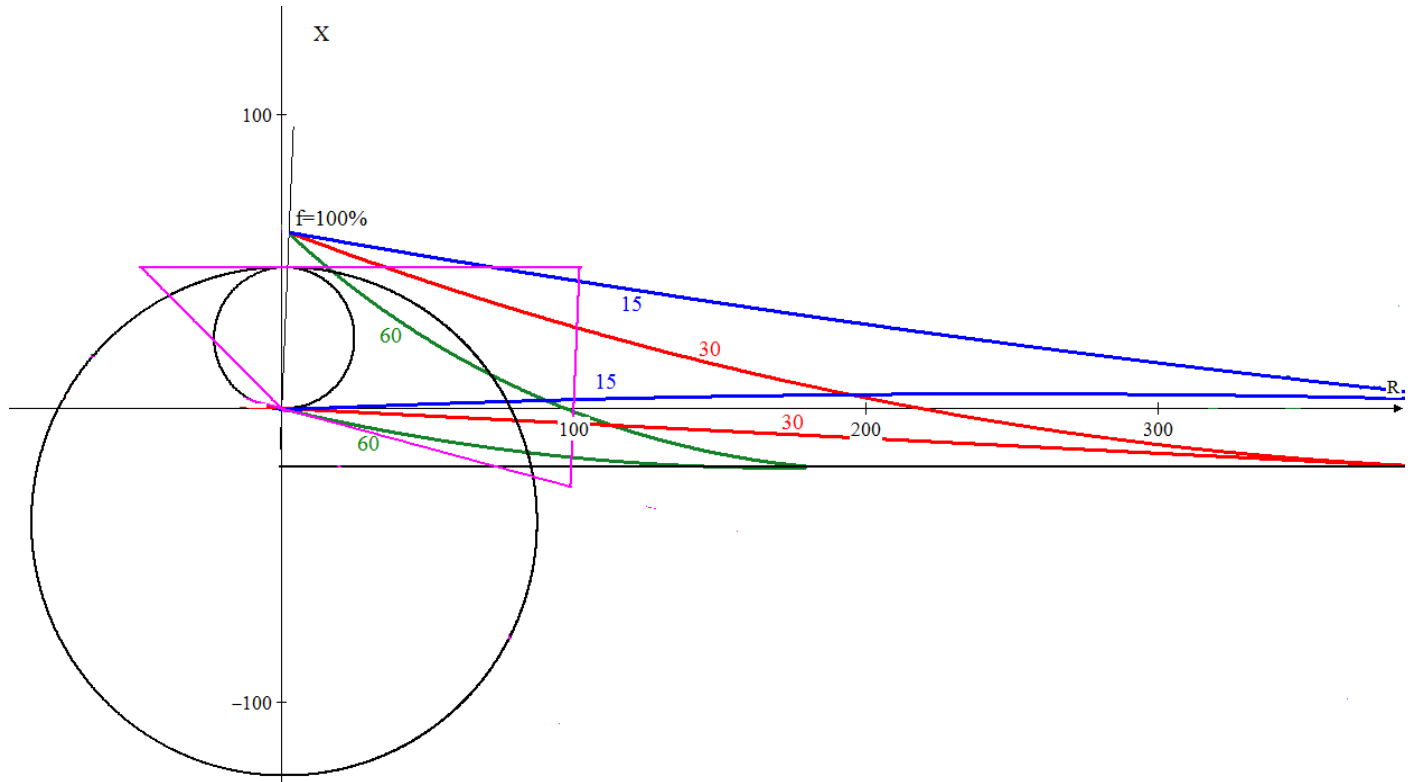


Figure 25: Impedance Loci for Weak Source Conditions, Swing Angles of  $15^\circ$ ,  $30^\circ$  and  $60^\circ$ , Terminal Faults.

The reaches correspond to the intersection points of the loci with the assumed relay characteristics, and are tabulated in Tables 1 and 2 for faults at remote and local terminals, respectively. Values of RF corresponding to threshold and operating regions are also shown. For example, at  $\delta=60^\circ$  and a fault at the remote terminal (100%), the relay set at 80% would misoperate for  $3.4\Omega < RF < 21.6\Omega$  and the quad for  $2.95\Omega < RF < 40.3\Omega$ , so the quad relay is less secure but has a higher fault resistance coverage for in-zone faults.

From Table 1 It is noted that when the swing line and the electrical center are behind the relay location the loci exhibit a very serious  $+\Delta R$  (underreach along the R axis) and a very high value of  $-\Delta X$  (overreach in X axis) so the relay seriously overreaches. This overreach is confined to internal faults on the line and the method of the study does not cover the behavior of the relay for faults on adjacent line(s), however, depending on the system parameters it can be observed that the relays could misoperate for faults on adjacent lines.

From Table 2 it is noted that with fault at the local terminal both  $\Delta R$  and  $\Delta X$  values are negative and the relays cover securely most of the terminal faults. For faults in the reverse direction relay operating principles are different and there is no problem of misoperation though the relays seem to have a reverse inductive reach.



Figure 26: Calculated Relay Reaches, Weak Source, Swing Angles of  $15^\circ$ ,  $30^\circ$  and  $60^\circ$ , Remote Terminal Fault.

**$m=100\%$  ,  $z1m=2.5+j60\Omega$**

angle $\delta$ degrees	Quad Reach		Mho ( expanded) reach	
	RF (actual)	Rapp	RF(actual)	Rapp
60	From: 2.95Ω	13.4-j12Ω	From 3.43Ω	15.4-j13.7Ω
	To: 40.3Ω	97.5-j61Ω	To: 21.6Ω	69-j48.4Ω
30	From 6Ω	33.5-j12Ω	NO OPERATION	
	To 21.6Ω	98.7-j32.5Ω		
15	From 12.2Ω	70.5-j12Ω	NO OPERATION	
	To 18Ω	99.3-j17Ω		

Table 1: Reach Calculations for Quad and Mho Characteristic, Fault at Remote Terminal  $m=100\%$ .

**m=0% , z1m=2.5+j60Ω**

Angle $\delta$ Degrees	Reactance		Mho (expanded)	
	RF (actual)	Rapp	RF(actual)	Rapp
60	From 0Ω	0Ω	From 0Ω	0Ω
	To 199.4Ω	99.3-j16.6Ω	To 143.3Ω	84.2-j15Ω
30	From 0Ω	0Ω	From 0Ω	0Ω
	To 117.3Ω	99.8-j5.1Ω	To 88.60Ω	80.4-j4.1Ω
15	From 0Ω	0Ω	From 0Ω	0Ω
	To 102.5Ω	100.1+j3.1	To 76.5Ω	77.2-j2.4Ω

Table 2: Reach Calculations for Quad and Mho Characteristics, Fault at Local Terminal, m=0%.

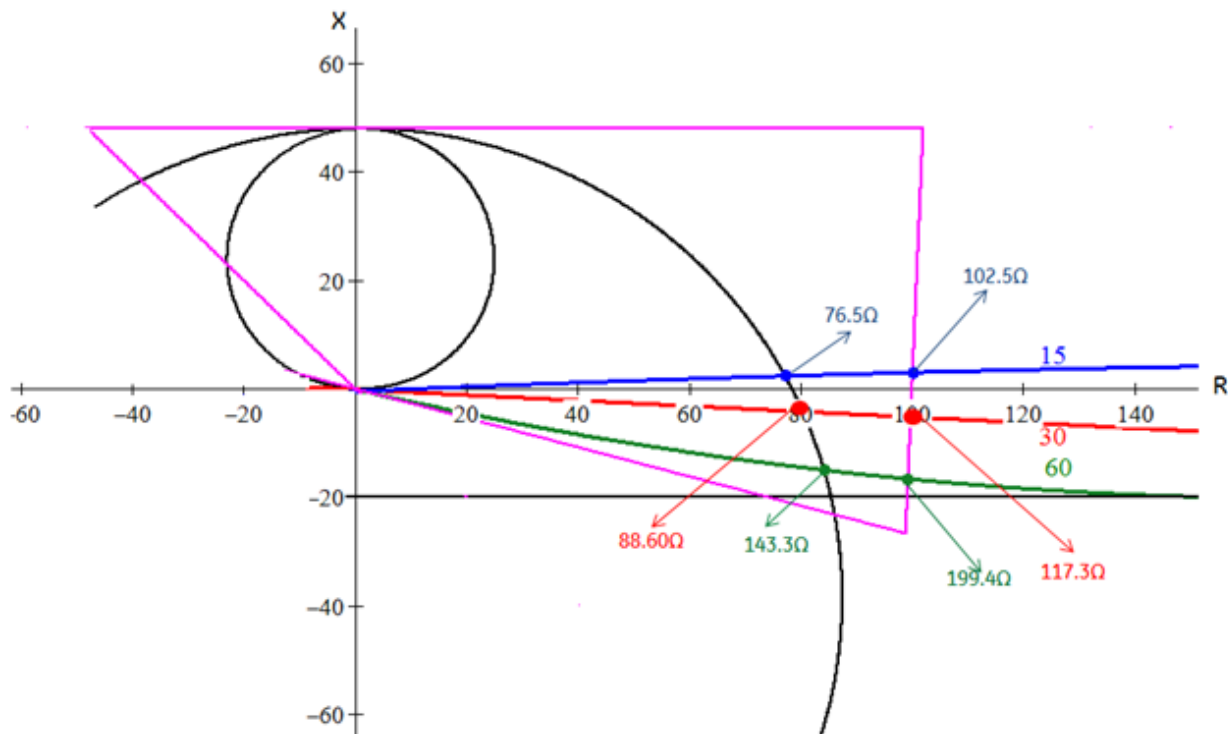


Figure 27: Calculated Relay Reaches Weak Source, Swing Angles of 15°, 30° and 60°, Local Terminal Faults.

## 7.2 Power imported at the local terminal

The studies were first made for swing angle,  $\delta$ , values of  $-30^\circ$  and  $-60^\circ$  for fault locations from 0 to 100%, in steps of 20%.

The results for  $\delta=-60^\circ$  are shown in Figure 28. It is clear that the relay underreaches very severely.

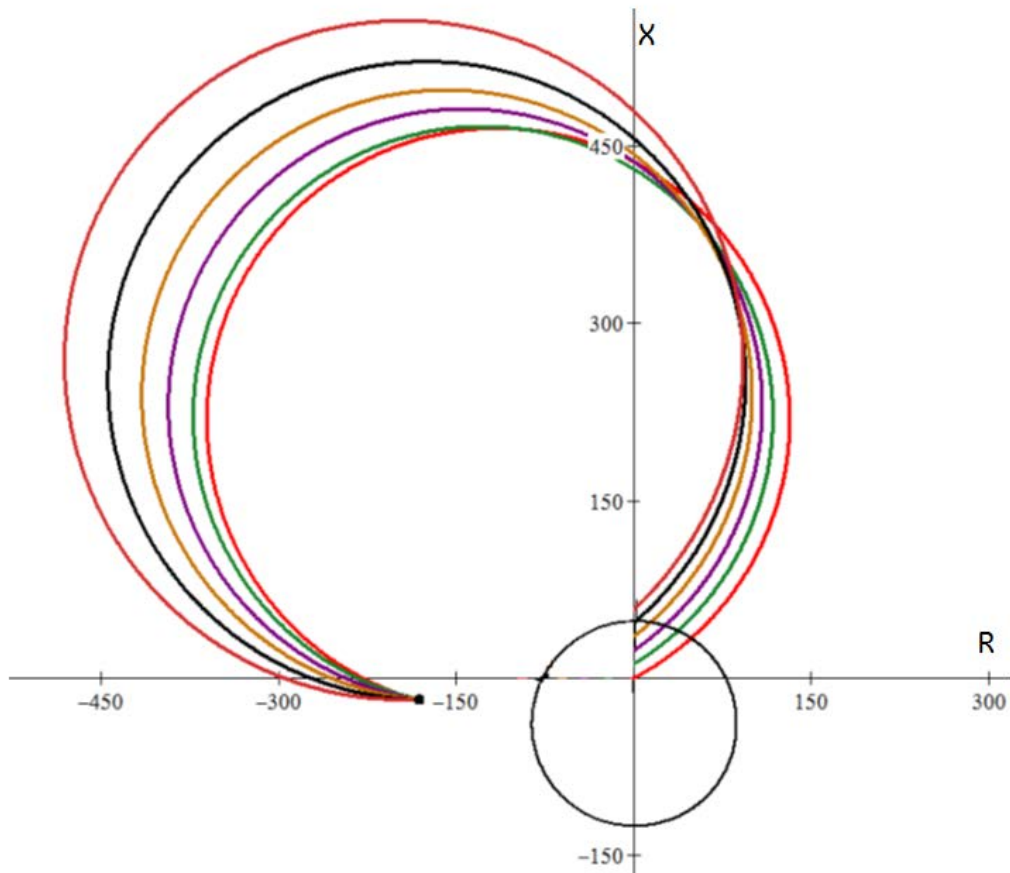


Figure 28: Impedance Loci for Weak Source Conditions,  $\delta=-60^\circ$ , Fault Distance in 20% Steps.

The points of intersection with the expanded mho operating characteristic are shown in Figure 29, the actual and apparent fault resistances are indicated in the Figure for each fault location. Both  $\Delta X$  and  $\Delta R$  values are positive, and the relay underreaches along both axes.

Similarly, reach calculations for  $\delta=-30^\circ$  are shown in Figure 30, the results are similar to  $\delta=-60^\circ$  but the underreach is not as severe.

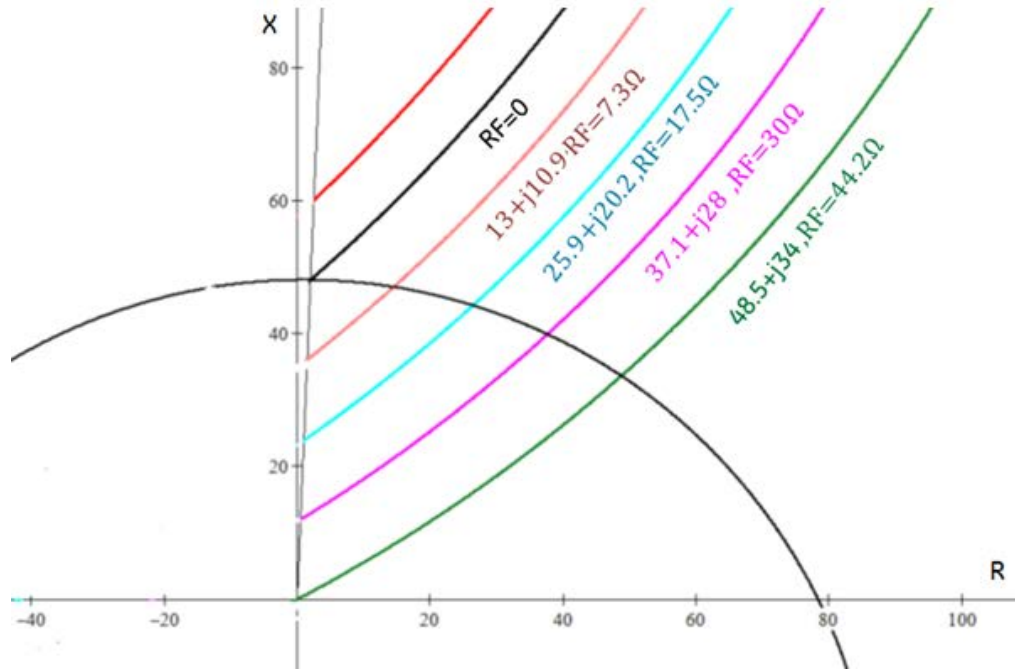


Figure 29: Calculated Relay Reaches, Weak Source,  $\delta = -60^\circ$ , Fault Distance in 20% Steps.

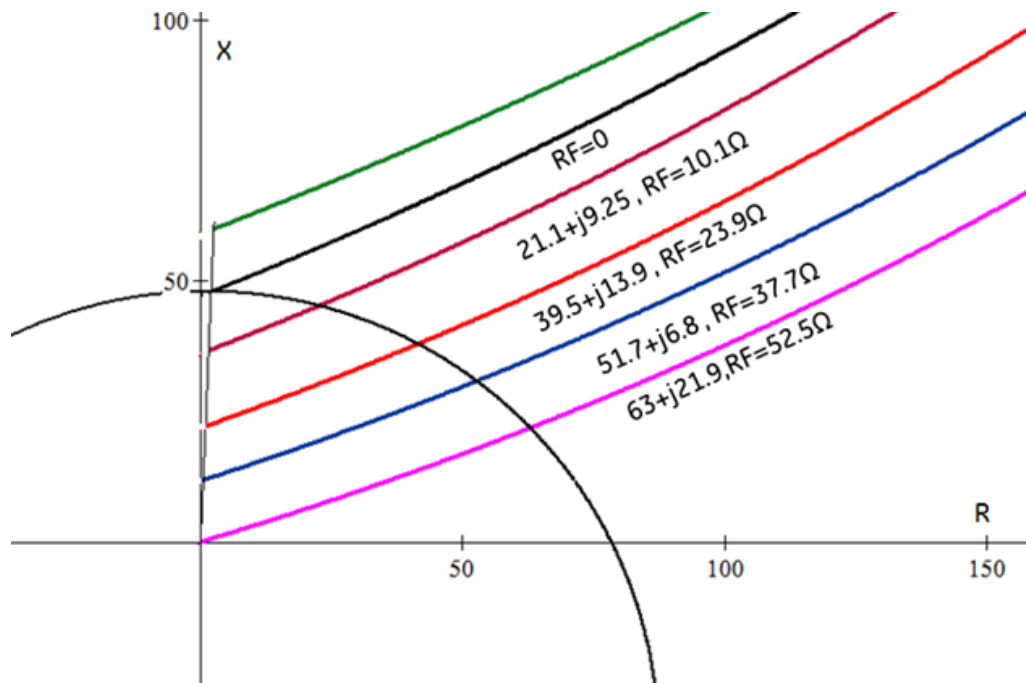


Figure 30: Calculated Relay Reaches, Weak Source,  $\delta = -30^\circ$ , Fault Distance in 20% Steps.

## 8 The Remote End Relay

Relays at the terminals of protection schemes communicate and a decision to trip is given in accordance, the main idea is to either permit tripping or to block tripping, therefore, a study on simultaneous measurement of relays at both ends provides very important information on the behavior of the overall scheme.

### 8.1 Working Impedance of the Remote End

With reference to Figure 12 redrawn in Figure 31 for both ends the working impedance for the remote end is calculated as;

$$Z' = \frac{V'}{I'} = \frac{V - I \cdot z_{1l}}{-I}$$

Or;

$$Z' = -Z + z_{1l} \quad (31)$$

For example, for one of the cases studied in the previous sections, with weak local source and  $\delta=60^\circ$  the local end working impedance was calculated as:

$$Z=182-j20\Omega$$

With the sample system line positive sequence impedance of:  $2.5+j60\Omega$  the remote end working impedance is;

$$Z'=-182+j20+2.5+j60= -179.5+j80\Omega$$

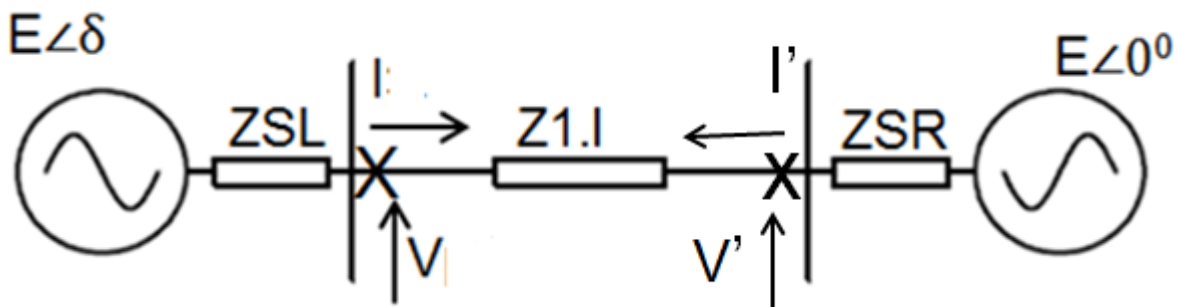


Figure 31: The Working Impedance for the Remote End.

Impedance loci for the relays at both ends are shown in Figure 32 for faults at both terminals, the mho expansion for each end has been taken into account by employing corresponding source impedances.

The relay reaches for this case is shown in Figure 33, it is noted that local fault location of 100% corresponds to remote distance of 0% and vice versa.

It can be seen that for a fault at the remote terminal (100% line length at local and 0% from remote) local relay set at 80% would overreach and operate for  $3.4\Omega < R_F < 21.6\Omega$ , other reaches can be seen in Figure 33.

Similar drawings are included for  $\delta = -60^\circ$  in Figure 34 and 35.

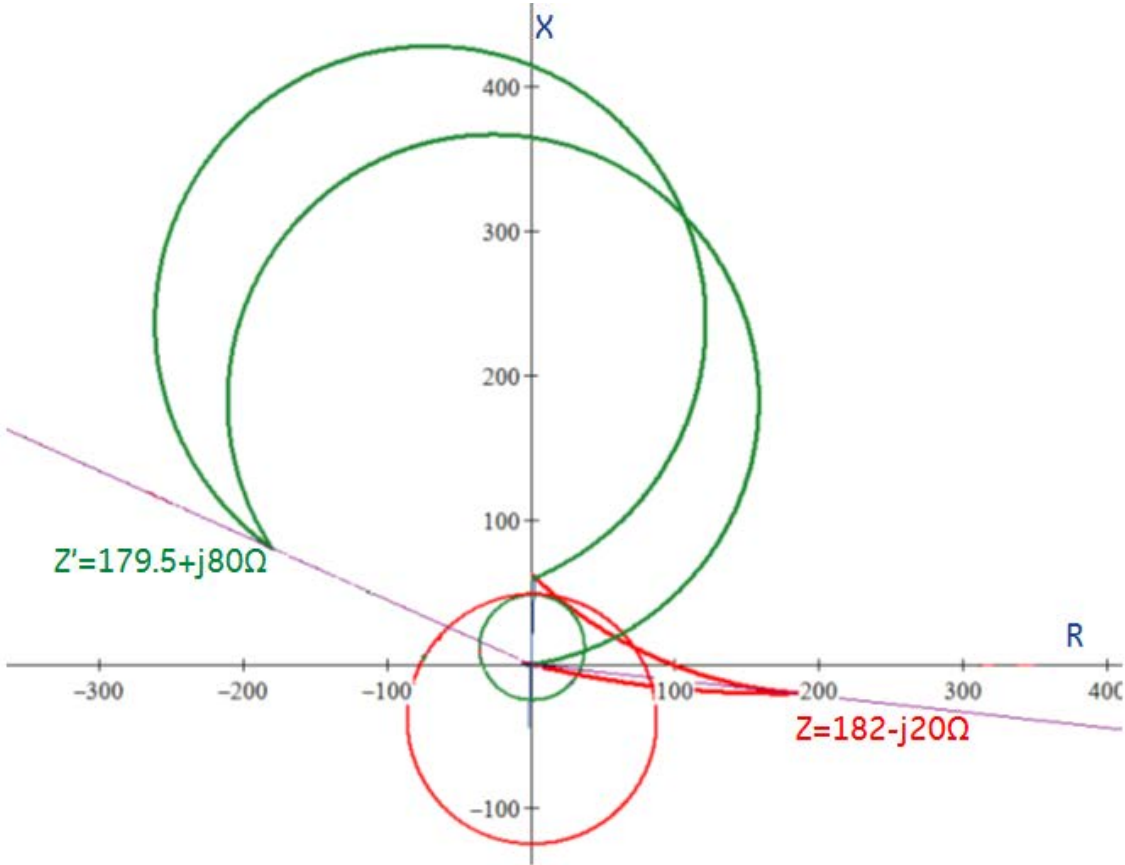


Figure 32: Impedance Loci for Both of the Ends, Weak Local Source and  $\delta = 60^\circ$ , Faults at Terminals.

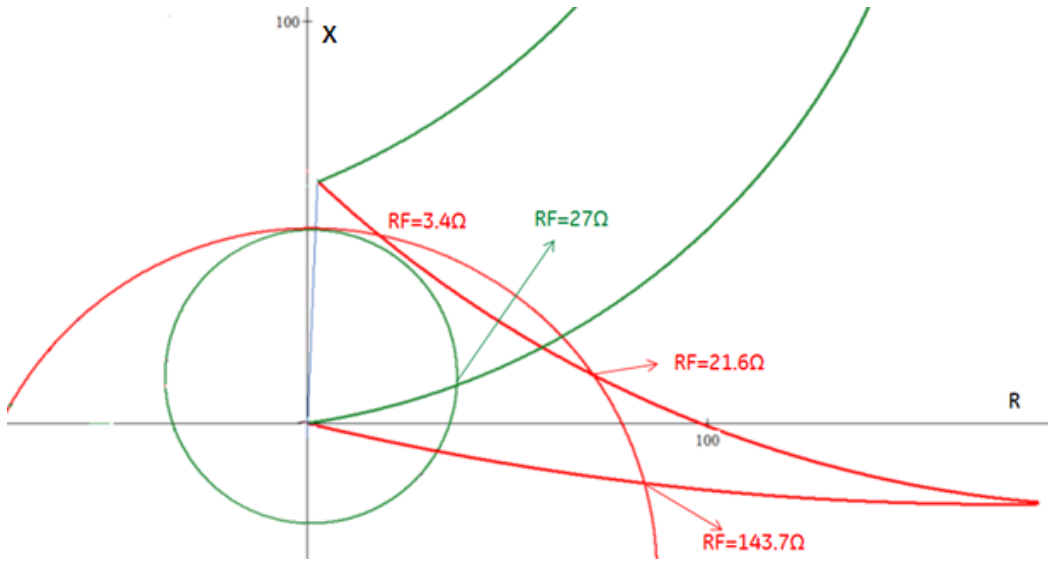


Figure 33: Relay Reach Calculations for Both of the Ends, Weak Local Source and  $\delta=60^\circ$ , Faults at Terminals.

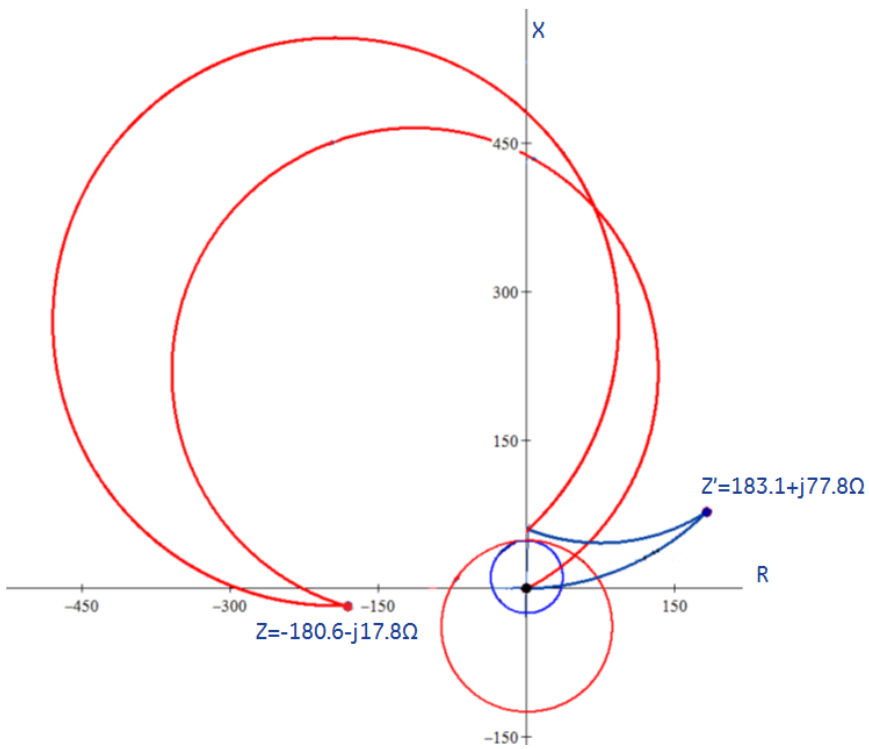


Figure 34: Impedance Loci for Both of the Ends, Weak Local Source and  $\delta=-60^\circ$ , Faults at Terminals.



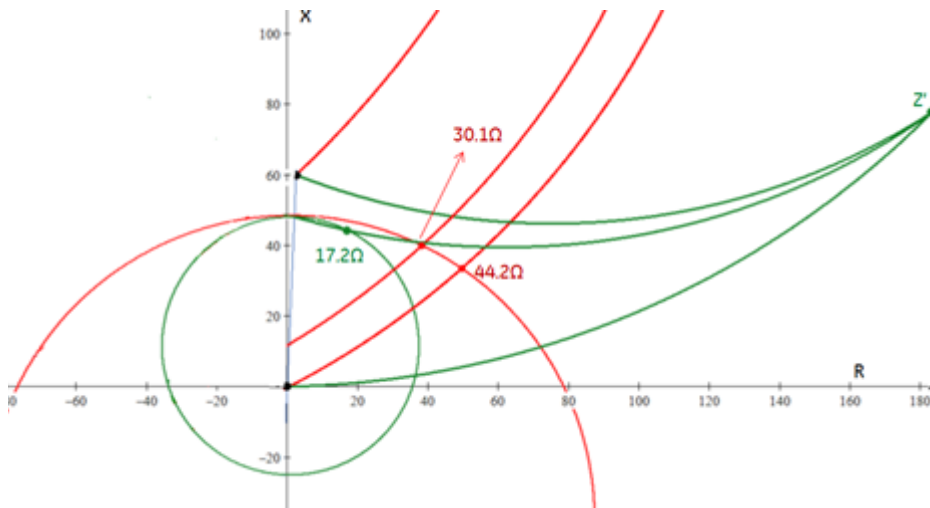


Figure 35: Relay Reach Calculations for Both of the Ends, Weak Local Source and  $\delta=-60^\circ$ , Faults at Terminals and 80% from Terminals (i.e. 20% from Remote Terminals).

It may be desired to fix the positions of the working impedance (pole K), and the location of the fault on the line (pole L) on the R-X plane, and analyze the two-ended operating conditions of both of the terminal relays on this plane. From Equation 31, it can be concluded that if we introduce a second R-X coordinate system onto the same impedance plane but rotate it by  $180^\circ$  with respect to the regular coordinates, to obtain  $-Z$ , and shift it by  $z_{11}$  to get  $Z'$ , we can display both ends with pole positions fixed at the same location and applicable to both terminal relays (Figure 36). We will call this system representation as **mono-planar bi-coordinate system**.

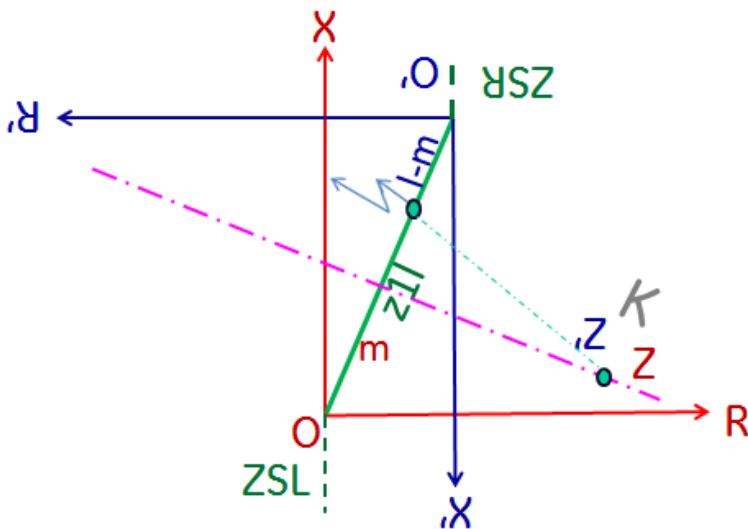


Figure 36: Mono-Planar Bi-Coordinate (?) System.

An example of this representation is shown in Figure 37 and 38 for weak source conditions,  $\delta=60^\circ$  and  $\delta=-60^\circ$ , respectively. A closer view of Figure 38 is shown in Figure 39.

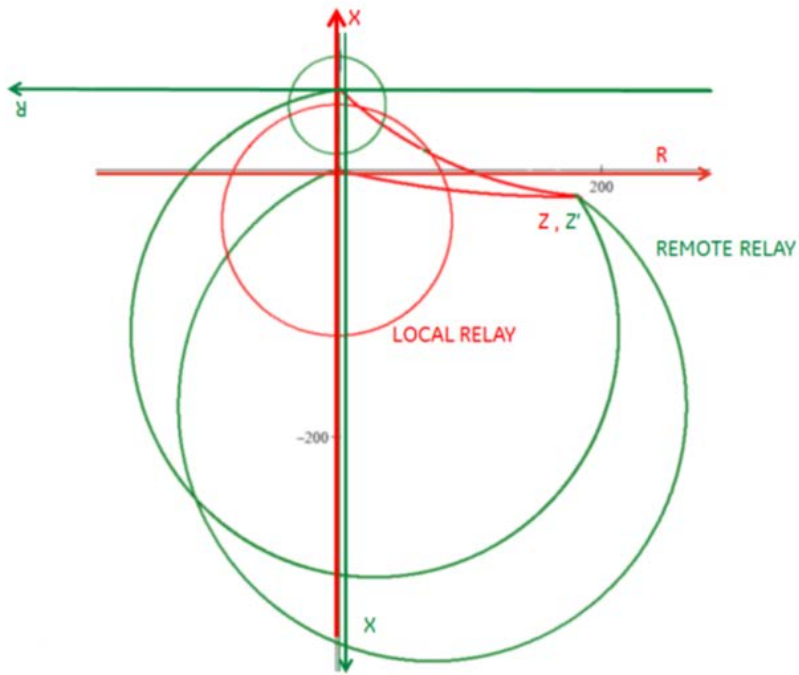


Figure 37: Bi-Coordinate Impedance Loci for Both ends, Weak Local Source and  $\delta=60^\circ$ , Faults at Terminals.

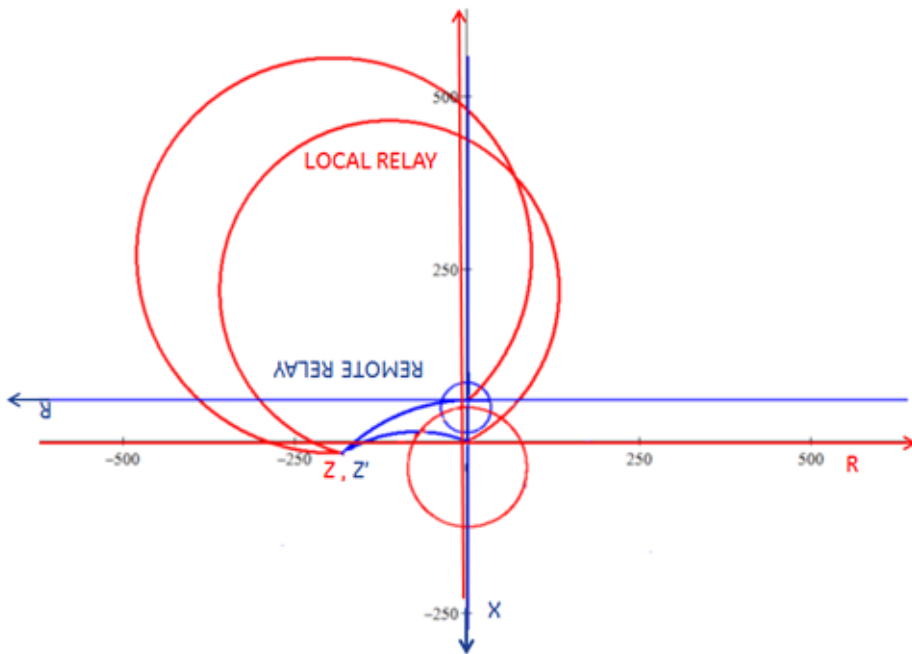


Figure 38: Bi-Coordinate Impedance Loci for Both Ends, Weak Local Source and  $\delta=-60^\circ$ , Faults at Terminals.

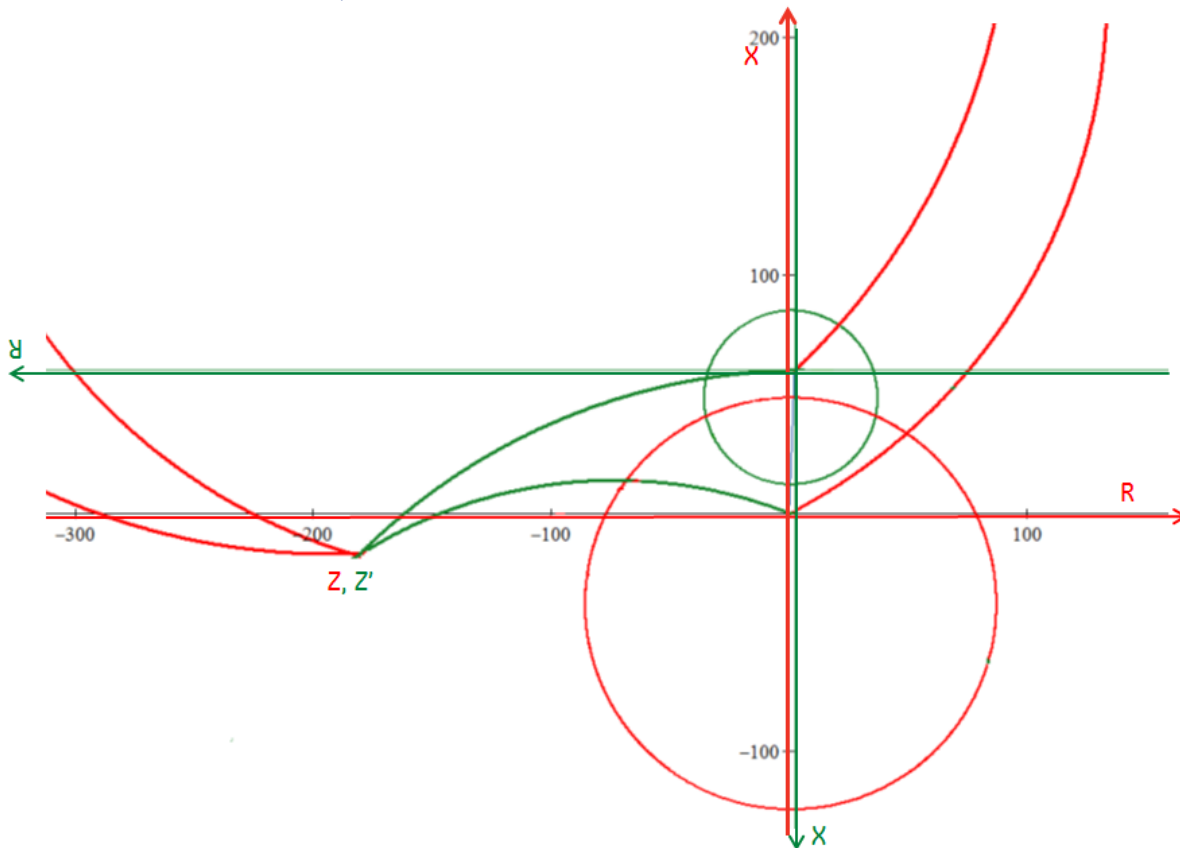


Figure 39: Bi-Coordinate Impedance Loci for Both Ends, Weak Local Source and  $\delta=-60^\circ$ , Faults at Terminals, Zoomed.

## 9. Conclusions

Determination of the effects of load current and fault resistance on the relay operation has always been a subject of great interest for protection engineers. The task of calculating, or at least accounting for, the fault resistance from single end quantities has also been a challenge in the design of relays, their operating principles and choice of relay characteristics as well as correct location of faults.

Various operating characteristics have been developed to cover large areas of fault resistance (quad and reactance characteristics) and methods are employed to reduce their effects (impedance measurement at zero crossing of local zero or negative sequence currents) and, still retain the stability of the relay under overloads or abnormal operation conditions (special characteristics like keyhole or use of blinders).

The correct choice requires a good knowledge of the factors influencing the relay measurement under different fault and operating conditions.

In this paper, a method is developed to calculate the impedances seen by the relays and to prove that the locus is an arc of a circle as the fault resistance is varied. The location of the centers and radii

depends on system and fault parameters. The tips of the loci arcs are defined by two poles L and K, where L corresponds to the point of fault on the line and K to working impedance.

The object of the paper was to introduce the problem to the engineers and give them simple tools to calculate possible behavior of relays under different operating and fault conditions, the loci can be calculated very easily ( in fact all calculations are based on high school mathematics ), and , the results obtained in a very short time using a very simple calculation program.

The working impedance, K pole of the loci, is a known quantity from pre-fault measurements (memory), or even under single phase to ground faults (e.g. A-phase) it could be approximated as the measurement of the cross relay (i.e.  $Z=V_{BC}/I_{BC}=Z_{BC}$ , measurement of B-C phase fault relay, this approximation would be precise if the positive and negative sequence source impedances are equal).

The other pole of concern, L, the point of fault on the protected line, could be chosen to correspond to the setting of the relay for reach calculations (i.e. 80%) to determine the operating area of the protection.

On the other hand, the analysis may assist relay designers choose adaptive methods of measurement or, algorithms most suited for high resistance ground faults as well as fault location techniques.

For low pre fault currents (with a small  $\delta$  swing angle and highly resistive Z),  $\varphi$  angle is about  $180^\circ$  for the exporting terminal, and  $0^\circ$  for the importing. Under these conditions the ZR loci would become straight lines through poles L and K as shown in Figure 40. Corresponding fault areas shown for power export and import.

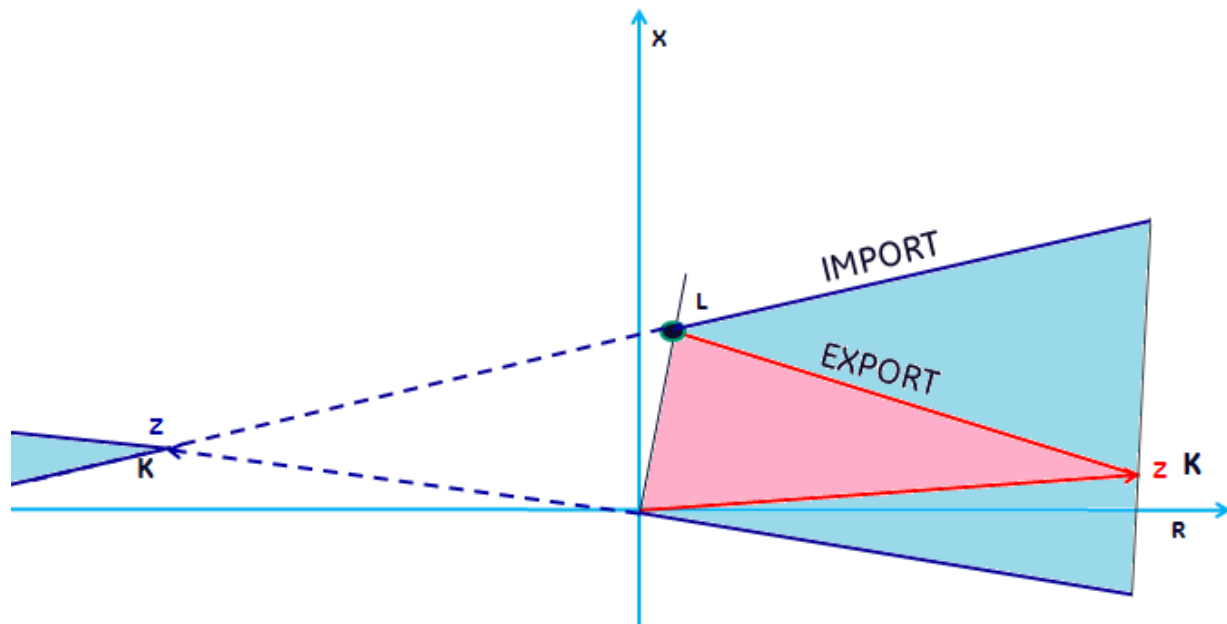


Figure 40: Measured Fault Impedance Areas with Z Highly Resistive.

A relay operating characteristic most suited to this area may be adopted for maximum coverage and stability. For example, as it is already known from the analysis in this paper the most severe cases would result for faults at the set reach of the relay. An optimum fault resistance coverage could probably be obtained by tilting the line reactance angle parallel to LK chord (L in this case would correspond to the relay setting e.g. 80%).

This assumption may not be applicable for faults during power swings where the swing angle  $\delta$  may have reached a high value. However could be effective for normal load transport cases where a stable operation condition may result in  $\delta$  values of 15-25°.

We did not go into recommending any settings and relaying techniques as distance relays have different operating methods and they can cope with the problem of high fault resistances in different ways. The relays working with phase comparator method may not have the quantities of concern readily available, while relays measuring the impedance of the fault loop by numerical methods and thereafter comparing these with the limits of operating zones may offer different methods of implementation.

As a final word, the task of protection engineers is to balance and maintain sensitivity and stability of operation under different conditions and, relays intended to UNDERREACH should never overreach the adjacent circuits, and those intended to OVERREACH should always do so for all fault and operating conditions. The influencing values  $\Delta X$  and  $\Delta R$  are easily calculated, the cases which cannot be covered by distance relays should be protected by a complementary DEF (directional earth fault) scheme.

## Biography

**Sinan Saygin** received his B.Sc. and M.Sc. degrees in Electrical Engineering at Middle East Technical University, Ankara in 1968 and 1969.. In 1968 he joined TEK ( Turkish Electricity Authority) as Protection and Measurement Specialist. He has worked in SCECO West, Saudi Arabia, as Substations Project Manager during 1980- 1982. In 1982 he joined ALSTOM as a technical consultant, and has worked in different positions. His works included series compensated line protection applications and design, distance relay numerical algorithms, marketing and applications in global scale. He has moved to USA in 2000 and worked as an Application Engineer in the Western Region. In 2012, he joined GE, and currently works as an Application Engineer in the Western Region. He is an active member of PSRC and IEEE.

**Zhiying Zhang** received his B.Sc. and M.Sc. degrees from the North China Institute of Electric Power (now North China Electric Power University-NCEPU) and a Ph.D. degree from the University of Manitoba, Canada, all in Electrical Engineering. He has over 25 years of working experience with electric utilities and with relay manufactures in various technical positions. Since 2007 he has been with General Electric, and currently holds the position of principal applications engineer at GE Digital Energy in Markham, Ontario. Zhiying is a registered professional engineer in the province of Ontario and a senior member of IEEE.

**Iliia Voloh** received his Electrical Engineering degree from Ivanovo State Power University, Russia. After graduation he worked for Moldova Power Company for many years in various progressive roles in Protection and Control field. He is currently an applications engineering manager with GE Multilin in Markham Ontario, and he has been heavily involved in the development of UR-series of relays. His areas of interest are current differential relaying, phase comparison, distance relaying and advanced communications for protective relaying. Iliia authored and co-authored more than 20 papers presented at major North America Protective Relaying conferences. He is an active member of the PSRC, and a senior member of the IEEE.

## References

- [1] J. Zydanowicz , Application of The Idea of Steady-State Impedance and Admittance to the Construction of Diagrams Intended for Analysis of the Operation of Distance and Directional Relays and Protective Schemes, CIGRE 1960.
- [2] Power Swing and Out-of-Step Considerations on Transmission Lines, IEEE PSRC , Working Group D6, Guide.
- [3] A. R. Van C. Warrington, Graphical Method for Estimating the Performance of Distance Relays During Faults and Power Swings, Trans. AIEE , 1949.
- [4] E. Clarke , Impedances Seen by Relays During Power Swings With or Without Faults , Trans. AIEE , 1945.
- [5] G.E. Alexander, J.G. Andrichak, W.Z. Tyska, S.B. Wilkinson , Effects of Load Flow on Relay Performance , GE-MULTILIN Publication GER-3743
- [6] Sinan Saygin, Effects of Load Current on the Impedances Presented to Distance Relays, M. Sc. Thesis Middle East Tech. University , Ankara, Turkey, 1969